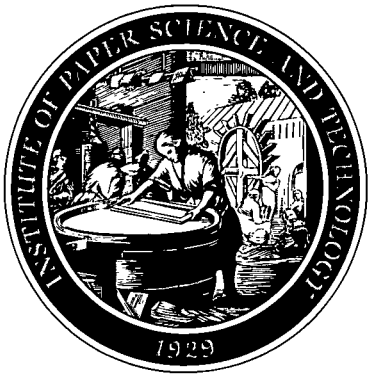

Institute of Paper Science and Technology

STATUS REPORTS

To The

CORROSION CONTROL

PROJECT ADVISORY COMMITTEE

April 29, 1993

IPST

Atlanta, Georgia

INSTITUTE OF PAPER SCIENCE AND TECHNOLOGY
PURPOSE AND MISSION STATEMENT

The Institute of Paper Science and Technology is a unique organization whose charitable, educational, and scientific purpose evolves from the singular relationship between the Institute and the pulp and paper industry which has existed since 1929. The purpose of the Institute is fulfilled through three missions, which are:

- to provide high quality students with a multidisciplinary graduate educational experience which is of the highest standard of excellence recognized by the national academic community and which enables them to perform to their maximum potential in a society with a technological base; and
- to sustain an international position of leadership in dynamic scientific research which is participated in by both students and faculty and which is focused on areas of significance to the pulp and paper industry; and
- to contribute to the economic and technical well-being of the nation through innovative educational, informational, and technical services.

ACCREDITATION

The Institute of Paper Science and Technology is accredited by the Commission on Colleges of the Southern Association of Colleges and Schools to award the Master of Science and Doctor of Philosophy degrees.

NOTICE AND DISCLAIMER

The Institute of Paper Science and Technology (IPST) has provided a high standard of professional service and has put forth its best efforts within the time and funds available for this project. The information and conclusions are advisory and are intended only for internal use by any company who may receive this report. Each company must decide for itself the best approach to solving any problems it may have and how, or whether, this reported information should be considered in its approach.

IPST does not recommend particular products, procedures, materials, or service. These are included only in the interest of completeness within a laboratory context and budgetary constraint. Actual products, procedures, materials, and services used may differ and are peculiar to the operations of each company.

In no event shall IPST or its employees and agents have any obligation or liability for damages including, but not limited to, consequential damages arising out of or in connection with any company's use of or inability to use the reported information. IPST provides no warranty or guaranty of results.

CORROSION CONTROL

ANNUAL RESEARCH REVIEW

APRIL 29, 1993

INSTITUTE OF PAPER SCIENCE AND TECHNOLOGY
500 10TH STREET, N.W.
ATLANTA, GEORGIA 30318

RECOVERY BOILER CORROSION

PROJECT 3628

Jeffery A. Colwell
Gregory J. Fonder

ANNUAL RESEARCH REVIEW
APRIL 29, 1993

INSTITUTE OF PAPER SCIENCE AND TECHNOLOGY
500 10TH STREET, N.W.
ATLANTA, GA 30318

TECHNICAL PROGRAM REVIEW

PROJECT TITLE: RECOVERY BOILER CORROSION

PROJECT CODE: CORRN

PROJECT NUMBER: 3628

DIVISION: Chemical and Biological Sciences

PROJECT STAFF: Jeff Colwell, Greg Fonder

FY 92-93 BUDGET: $116,000

GOAL:

Improve safety and increase operating life of equipment by proper selection of construction materials and by identifying suitable process conditions.

OBJECTIVE:

To understand the causes of corrosion on the waterwall tubes in the lower furnace of kraft recovery boilers.

SUMMARY:

This project is focused on two main areas of corrosion in the lower furnace of the recovery boiler: fireside corrosion and corrosion due to hydroxide condensation at ports. Our understanding of the gas-solid reactions leading to sulfidation of carbon steel tubes has improved with the knowledge of how specific components of the gas impact kinetics. For example, at constant sulfur pressure, the influence of water vapor does not appear to be large. Moreover, it appears that a correlation with oxygen or sulfur dioxide exists, and that at a critical level the kinetics dramatically increase. Our experimental methods are being modified to merge with those being proposed by AFPA so that future data can be directly used by other laboratories.

The need for sensor development is still identified as an important need for furthering our understanding of gas-solid reactions in the recovery boiler. Solid electrolytes based on sulfates offer one possible method, but only provide information on the product of sulfur and oxygen activities. To arrive at a useful measurement of the

conditions will require additional independent knowledge of either the sulfur or oxygen activity. Additional efforts this year were spent trying to identify methods to utilize zirconia oxygen sensors at low temperatures, but were not successful. However, a new technique based on the use of AgI as a sulfur sensor may allow development of the sulfate sensors to go forward. This sensor will have a limited range of applicable sulfur pressures, but these values are expected to be close to those needed for recovery boilers.

The initial experiments by Lisa McMillian for her master's research concluded that the current apparatus for measuring continuous kinetics is not accurate. The deposition of components from the complex simulated furnace gas would not allow weight changes to be followed. A brief morphological investigation of the effect of preoxidation showed that at a higher oxygen pressure, the sulfidation kinetics appeared to be slower.

The previous report outlined a postulated mechanism for air port corrosion which was consistent with a number of observations. During last year a new apparatus was built which will facilitate the collection of oxide solubility data in molten hydroxides. An offer was made to a post-doctoral associate to work full-time on this task. He arrived in November, but did not have the proper immigration status, and could not be hired. This task was then taken on by a new Ph.D. student, Matt Estes, who successfully defended his proposal and began work in March of 1993.

INTRODUCTION

The main objective of this project is to understand the causes of corrosion on the waterwall tubes in the lower furnace of the kraft recovery boiler. Once those causes are better understood, it is expected that mitigation strategies can be developed which will have a sound basis. Problems on the fireside and coldside have been observed by many mills, and corrosion has been implicated in several smelt-water explosions over the years. Obviously, safe operation of the boiler is of prime concern, so IPST has been aggressively pursuing research which will contribute to the general, and specific, understanding of recovery boiler corrosion.

This project has been divided into several different tasks to focus our efforts on areas that need the most attention. Figure 1 gives an overview of the structure of the project and how it ties in with other related activities, such as student research and research funded by others. Next to each task in the figure is a brief description of the main objective or the question which needs to be answered.

REVIEW OF WORK COMPLETED IN 1991-1992

In the general area of gas-solid reactions, experiments were conducted in an effort to elucidate the effect of different components in the combustion gas on corrosion. Our standard experiments were conducted in 1% H_2S, 1% O_2, 2% H_2O, 10% CO_2, with the balance N_2. So, for example, the effect of water vapor was assessed by increasing from the initial amount from 2% to 9%. The additional water vapor did not cause any additional corrosion to carbon steel, but did increase stainless steel corrosion rates by a factor of 5. Apparently, 2% H_2O is above a threshold for carbon steel so that further increases do not affect the rates to any great extent. We also investigated an experimental pack cementation coating in our standard

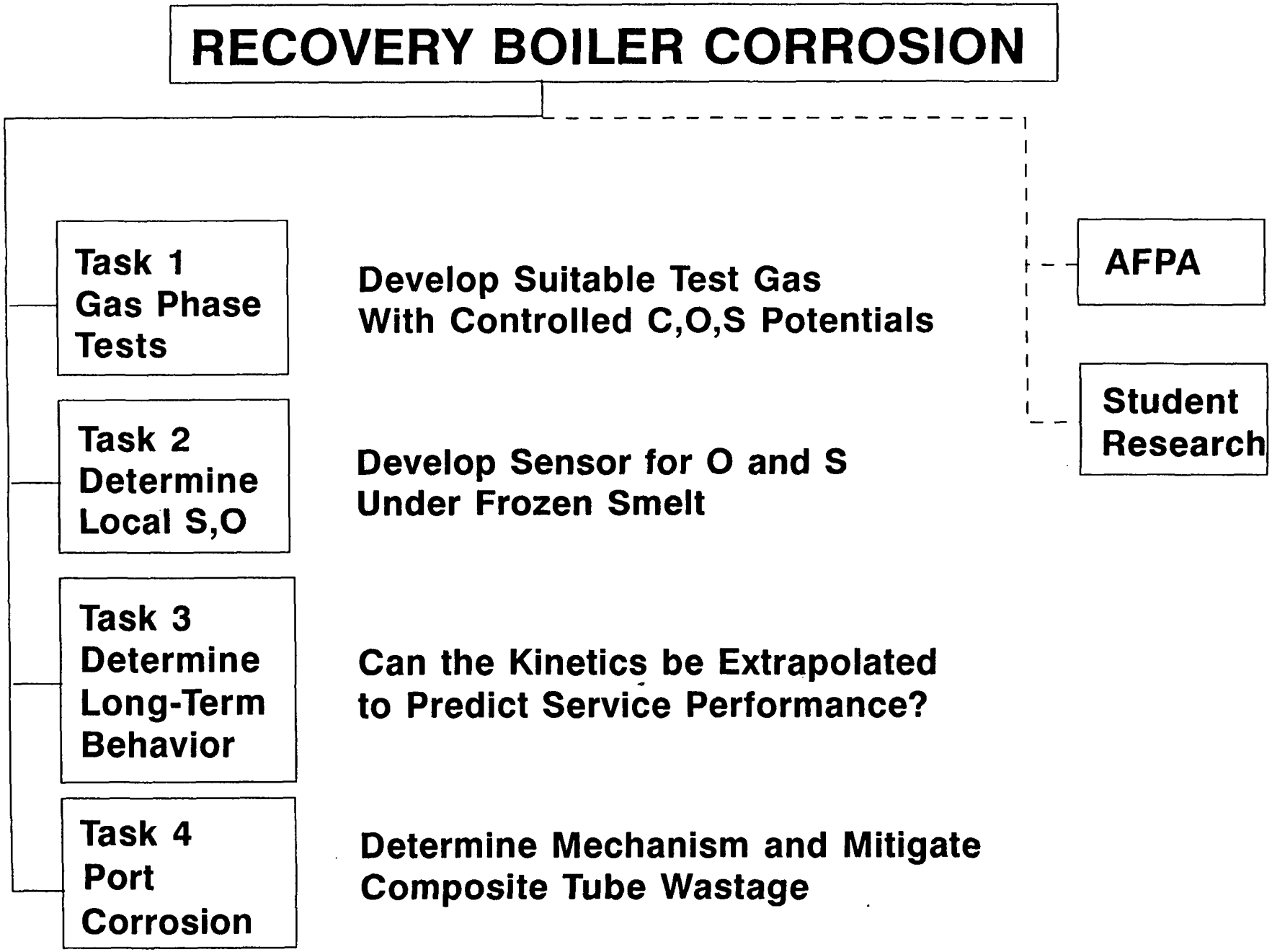

Fig. 1. Overall Organization of Recovery Boiler Corrosion Project

atmosphere. The Cr-Si coating, which is being developed at Ohio State University, performed well with a corrosion rate of less than 1 mpy over 168 hours at 440 °C.

Another task was concerned with trying to develop a concept to allow the local values of the partial pressures of oxygen and sulfur to be measured underneath frozen smelt. The concept is based on the use of solid electrolytes and requires the independent knowledge of the oxygen partial pressure to arrive at the sulfur partial pressure. An attempt was made to use stabilized zirconia as an oxygen sensor, but it was found that it would not function at temperatures below approximately 500 °C, presumably because of the onset of electronic conduction.

Last year a report was also made on the construction and calibration of an apparatus to determine the long-term kinetics of sulfidation. The apparatus was designed to record continuously the weight of a specimen versus time to allow the kinetics to be described without extrapolation. The calibration tests were done in air and compared favorably with results in the literature for similar tests.

Most of the effort reported last time was focused on the air port corrosion task. A number of electrochemical, weight-loss and field tests were covered, as well as a proposed theory for the mechanism. Consideration of all the data led us to conclude that the most likely cause, as has been reported elsewhere, was the presence of molten NaOH-based salts. A theory, based on the hot corrosion of nickel-base alloys in gas turbines was utilized to develop a theory of air port corrosion. As part of the theory, the high solubility of normally protective oxides present on stainless steel may explain the reason why stainless steel corrodes at a much faster rate than carbon steel in molten NaOH.

DISCUSSION OF 1992-1993 RESULTS

The discussion is organized to summarize the results separately for each task previously defined in Figure 1.

Task 1. Gas Phase Reactions

The premise of this task is that corrosion of waterwall tubes is a result of a reaction with gases which cause oxides and sulfides to form. If only iron oxides are formed, then the corrosion is minimal, but when iron sulfides form the kinetics are rapid which consumes the base metal at a rate much faster than desired. The presence of the frozen smelt layer does not directly cause corrosion, but reactions between it and gases which migrate through the layer can react to form an environment underneath the smelt which is quite different from the bulk gas in the furnace. Consequently, the local environment beneath the smelt will control the corrosion kinetics and tests which simulate that environment would be best to understand the corrosion mechanism. The standard IPST environment was selected to achieve several objectives, such as employing components representative of the combustion environment. In addition, the combination of oxygen and hydrogen sulfide in equal amounts has also been reported by others to maximize laboratory corrosion rates, so this was employed to accelerate the reactions and the acquisition of data.

Two types of experiments were conducted for this task. The first series was designed to determine the effect of the various components of a complex atmosphere and the second was designed to reproduce the procedures put forth by AFPA.

Effect of Gas Components

Based on the results obtained last year, a test matrix was developed to help determine which, if any, of the components in the standard IPST test gas have the most impact on corrosion. There were two reasons for this. First, if certain components could be identified as most influential, it may point to ways to slow corrosion by subsequent determination of how boiler operating parameters impact these critical environmental variables. Second, because AFPA-funded work is currently focused on developing a single oxidant test, it would be of use to determine the effect that various additions to that test gas have on corrosion so that directions for modification will be clear. In fact, it is expected that some of these variables will be examined in future AFPA projects, so the data generated here will be of use in supporting that project.

Procedures

A test matrix was designed to study the effect of various gas compositions on the corrosion of carbon steel coupons (AISI 1018) at nominally the same sulfur partial pressure. The reason for trying to keep the sulfur partial pressure constant was an attempt to link this work with the proposed AFPA test, which is a single oxidant test which is conducted at one partial pressure of sulfur. A software package (TEQWORKS®) was used to calculate the equilibrium gas composition for a given set of inlet conditions. By trial and error, various sets of initial conditions with a number of additions were determined to provide nominally a constant sulfur pressure. Of specific interest was the effect of water vapor, oxygen, and carbon dioxide. A summary of the test matrix is shown in Table 1, where the initial conditions are given along the top and left side of the matrix, and the partial pressures of sulfur and water vapor are given in the body of the matrix. There are other components which also form, but these are not listed in the table because of space limitations, and are instead given in Table 2.

Table 1. Initial Gas Compositions and Selected Equilibrium Values Corresponding to Corrosion Rates in mpy.

Vertical Furnace	Horizontal Furnace	Horizontal Furnace	Vertical Furnace	Horizontal Furnace	Horizontal Furnace
1.3% H_2S, balance N_2 (This test only) 0% H_2O added	1.3% H_2S, balance N_2 (This test only) 0% H_2O added	0% H_2O added	0% H_2O added	3% H_2O added	10% H_2O added
$Ps_2 = 2.08x10^{-5}$ $PH_2O = 0.0$ Area = 18.7 18.7 W.Loss = 23.2 20.5 Corr. Rt. = 4.5 4.0	$Ps_2 = 2.08x10^{-5}$ **A** $PH_2O = 0.0$ Area = 18.9 18.9 W.Loss = 27.8 27.4 Corr. Rt. = 5.4 5.3				
1.5% H_2S, balance N_2		$Ps_2 = 2.29x10^{-5}$ **B** $PH_2O = 0.0$ Area = 19.2 19.2 W.Loss = 26.1 30.0 Corr. Rt. = 5.0 5.7	$Ps_2 = 2.29x10^{-5}$ $PH_2O = 0.0$ Area = 18.9 18.6 W.Loss = 25.9 26.3 Corr. Rt. = 5.0 5.2	$Ps_2 = 2.11x10^{-5}$ **E** $PH_2O = 0.03$ Area = 18.7 18.6 W.Loss = 54.7 32.0 Corr. Rt. = 10.7 6.3	$Ps_2 = 1.37x10^{-5}$ **H** $PH_2O = 0.10$ Area = 18.9 18.6 W.Loss = 66.7 39.6 Corr. Rt. = 12.9 7.8
1.0% H_2S, 10% CO_2, balance N_2		$Ps_2 = 4.58x10^{-5}$ **C** $PH_2O = 1.33x10^{-3}$ Area = 19.5 18.4 W.Loss = 48.1 49.2 Corr. Rt. = 9.0 9.8	$Ps_2 = 4.58x10^{-5}$ $PH_2O = 1.33x10^{-3}$ Area = 18.7 19.2 W.Loss = 47.2 48.8 Corr. Rt. = 9.2 9.3	$Ps_2 = 1.65x10^{-5}$ **F** $PH_2O = 0.03$ Area = 18.7 18.6 W.Loss = 56.8 46.9 Corr. Rt. = 11.1 9.2	$Ps_2 = 8.52x10^{-6}$ **I** $PH_2O = 0.10$ Area = 18.6 18.6 W.Loss = 65.1 49.9 Corr. Rt. = 12.8 9.8
0.7% H_2S, 1.0% O_2, 10% CO_2, balance N_2		$Ps_2 = 1.02x10^{-4}$ **D** $PH_2O = 6.84x10^{-3}$ Area = 18.6 18.6 W.Loss = 91.2 50.4 Corr. Rt. = 17.9 9.9	$Ps_2 = 1.02x10^{-4}$ $PH_2O = 6.84x10^{-3}$ Area = 18.7 18.6 W.Loss = 59.4 59.4 Corr. Rt. = 11.6 11.7	$Ps_2 = 2.67x10^{-5}$ **G** $PH_2O = 2.98x10^{-2}$ Area = 18.9 18.6 W.Loss = 104.1 107.4 Corr. Rt. = 20.1 21.1	$Ps_2 = 6.08x10^{-6}$ **J** $PH_2O = 0.10$ Area = 18.6 18.6 W.Loss = 111.8 126.4 Corr. Rt. = 23.4 24.8

The gas flow rate for all tests is 6 L/hr. The test temperature is 360°C. All tests last for 5 days. Area is in cm^2, weight loss in mg, and the corrosion rate in mpy.

Table 2. Equilibrium Gas Concentrations for Initial Gas Mixtures Given in Table 1.

Gas	SH	H_2	H_2S	NH_3	CO	CO_2	COS	O_2	SO	SO_2
A	1.33×10^{-10}	4.16×10^{-5}	1.30×10^{-2}	3.25×10^{-9}	0.0	0.0	0.0	0.0	0.0	0.0
B	1.47×10^{-10}	4.58×10^{-5}	1.50×10^{-2}	7.51×10^{-9}	0.0	0.0	0.0	0.0	0.0	0.0
C	1.33×10^{-10}	1.87×10^{-5}	8.65×10^{-3}	1.87×10^{-9}	7.30×10^{-5}	9.87×10^{-2}	1.25×10^{-3}	4.61×10^{-32}	0.0	3.47×10^{-8}
D	2.37×10^{-11}	2.68×10^{-7}	1.85×10^{-4}	3.20×10^{-12}	2.08×10^{-7}	0.10	5.33×10^{-6}	5.94×10^{-27}	1.12×10^{-10}	6.61×10^{-3}
E	1.44×10^{-10}	4.77×10^{-5}	1.50×10^{-2}	7.87×10^{-9}	0.0	0.0	0.0	3.61×10^{-30}	1.26×10^{-12}	1.83×10^{-6}
F	1.10×10^{-10}	3.57×10^{-5}	9.90×10^{-3}	4.82×10^{-9}	6.25×10^{-6}	0.10	6.45×10^{-5}	6.44×10^{-30}	1.50×10^{-12}	2.91×10^{-6}
G	2.14×10^{-10}	8.33×10^{-7}	2.94×10^{-4}	1.73×10^{-11}	1.48×10^{-7}	0.10	1.94×10^{-6}	1.17×10^{-26}	8.07×10^{-11}	6.67×10^{-3}
H	1.29×10^{-10}	5.93×10^{-5}	1.50×10^{-2}	1.05×10^{-8}	0.0	0.0	0.0	2.59×10^{-29}	2.72×10^{-12}	1.06×10^{-5}
I	9.35×10^{-11}	4.99×10^{-5}	9.95×10^{-3}	7.66×10^{-9}	2.63×10^{-6}	0.10	1.95×10^{-5}	3.66×10^{-29}	2.55×10^{-12}	1.18×10^{-5}
J	1.55×10^{-11}	1.93×10^{-6}	3.25×10^{-4}	5.82×10^{-11}	1.02×10^{-7}	0.10	6.39×10^{-7}	2.45×10^{-26}	5.58×10^{-11}	6.68×10^{-3}

Standard flat test coupons (AISI 1018) which were 3" x 3/4" x 1/8" were obtained from Metal Samples Co. A 3/4" piece was cut off one end and also exposed to the environment to allow for metallographic examination at the conclusion of the test in addition to the weight loss determination on the remainder of the coupon. The surface preparation of the coupons consisted of burnishing in a tumbler for 48 hours using triangular-45° coarse cut ceramic media (McMaster-Carr #4918A29). After burnishing the specimens were cleaned in acetone and stored in a desiccator until needed.

The gas flow rate for all tests was 6 L/hr, the test temperature was 360°C and the test duration was 5 days. The furnace configuration was both horizontal and vertical as indicated in Table 1. For the horizontal runs, the specimens were placed in a ceramic boat and pushed into the center of the furnace while nitrogen gas flowed through the furnace. After a 15 minute purge, the temperature was raised to 360°C and then the proper gas mixture was introduced. At the end of the 5-day period, the gas mixture was interrupted and replaced with flowing nitrogen and the furnace was allowed to cool overnight before removing the specimens. The metallographic specimens were then prepared and photographed and the weight loss specimens were glass bead blasted to allow the corrosion rates to be calculated.

Results

The corrosion rates for each test in mpy are also given in Table 1 for each experiment. Figures 2 through 4 show the corrosion rate versus oxygen, mercaptan and sulfur dioxide, respectively. As can be seen, the corrosion rate is fairly constant until the oxygen partial pressure is increased to about 10^{-26}atm, at which the rate increases rapidly with increasing oxygen. Figure 3 gives the same information, but versus mercaptan and it can be seen that an inverse relationship holds. That is, increasing mercaptan at nominally constant sulfur pressure correlates with a decrease in corrosion rate. The next figure, Figure 4, shows the effect of SO_2, which is similar to the oxygen effect, as would be expected. A number of other correlations were attempted, but no trends could be observed.

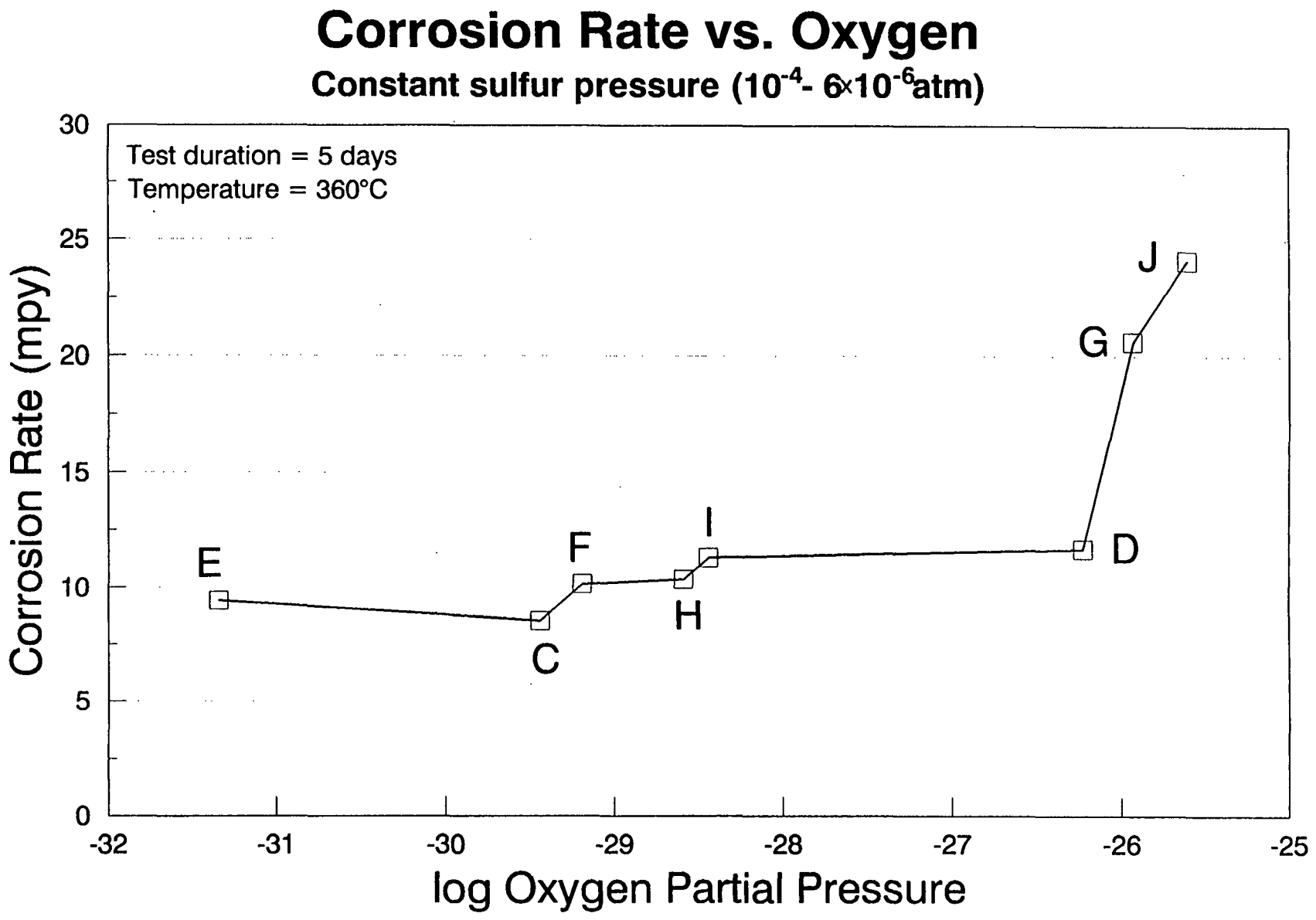

Fig. 2. Corrosion Rate vs. Oxygen for Constant Sulfur Partial Pressure

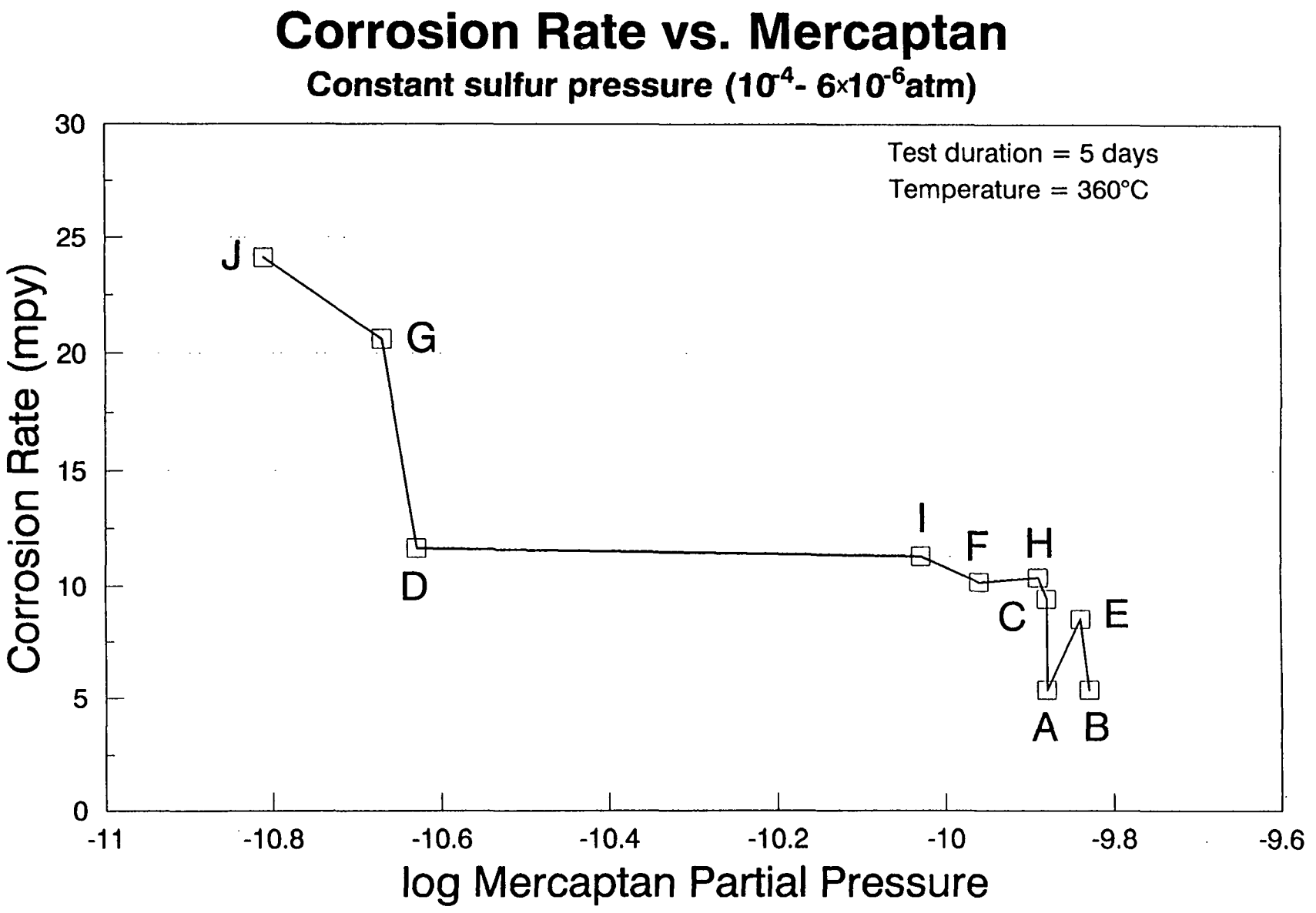

Fig. 3. Corrosion Rate vs. Mercaptan for Constant Sulfur Partial Pressure

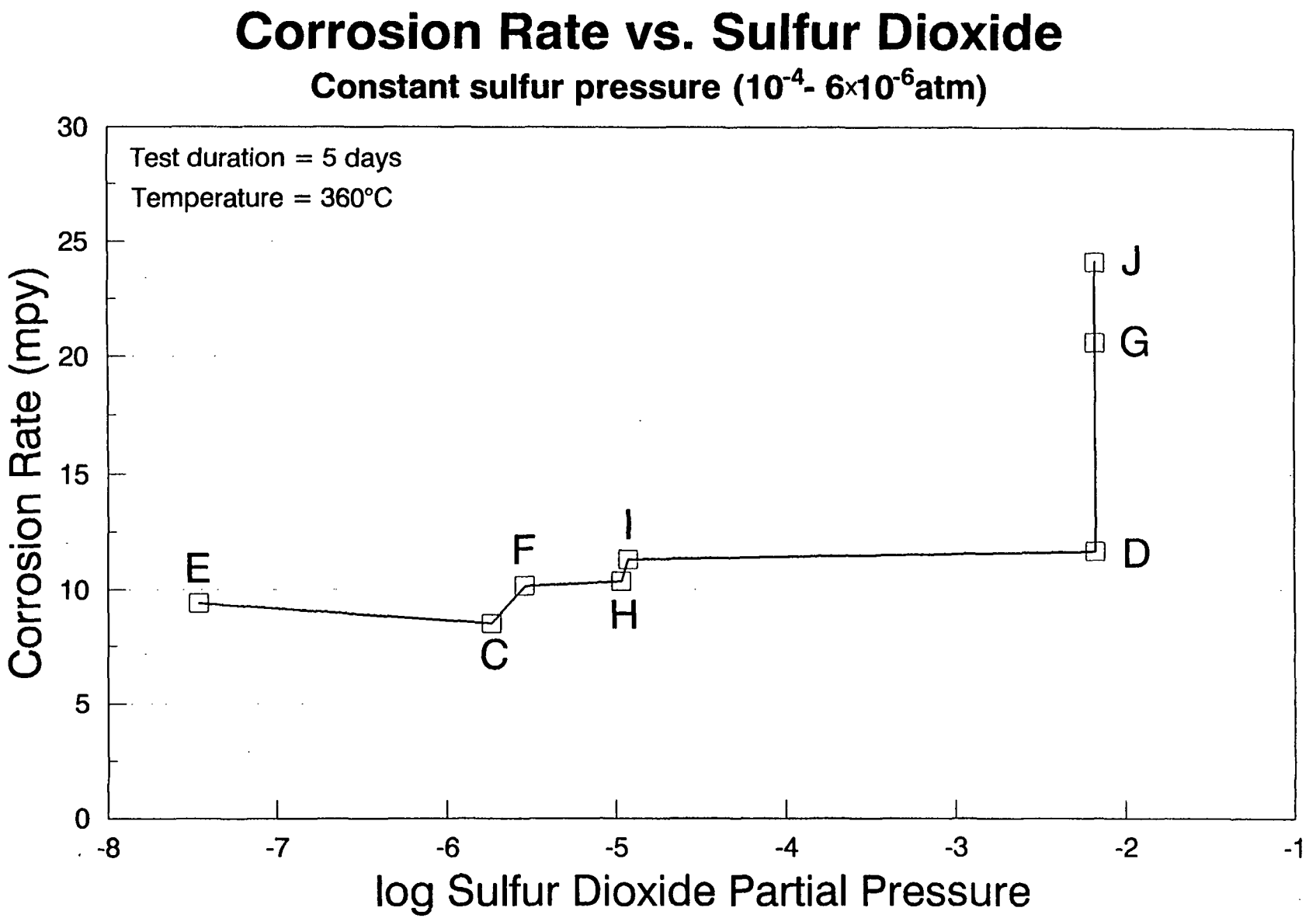

Fig. 4. Corrosion Rate vs. Sulfur Dioxide for Constant Sulfur Partial Pressure

The data in Table 1 can be placed in three general categories depending upon corrosion rate. There seem to be 3 groups of data: about 5 mpy, about 10 mpy and about 20 mpy. These groups can be plotted on the Fe-S-O phase stability diagram, which is shown in Figure 5. Note that boxes have been drawn to signify the range of environmental conditions corresponding to that approximate corrosion rate. As can be seen, the partial pressure of sulfur is almost constant over all 3 groups. Below each box are the letters corresponding to experiments shown in Table 1, and above each box is shown the range of water vapor. At the water vapor contents of this series of experiments there is overlap over all the corrosion rate ranges. Apparently water vapor has little incremental effect on the corrosion of carbon steel under these conditions. The oxygen effect can be easily seen, but also note that the SO_2 content also varies and has values between 10^{-15} and 10^{-2} atm. Perhaps the SO_2 concentration is the controlling factor in these environments.

Consequently, it has been found that the influence of water vapor at this single level of sulfur partial pressure is not very significant. The equilibrium calculations show that the addition of any oxygen containing gas (including CO_2) causes between 0.1 and 1 percent of water to form as a result of reaction with H_2S. The addition of water in the 3 to 10 percent range had little effect on corrosion rates; perhaps the presence of levels on the order of 0.1 percent is sufficient for the effect. The oxygen effect may be related to SO_2 formation and a simplified test using just SO_2 may be sufficient to rank and describe the corrosion behavior of carbon steels. More experimentation would be required before a final conclusion can be made.

AFPA Reproducibility Test

Previous work at IPST in this area used a horizontal tube furnace and a complicated gas designed to simulate a combustion environment, specifically, mixtures of various amounts of H_2S, CO_2, O_2, H_2, and H_2O were used in a N_2 carrier gas. Because AFPA is trying to develop standardized test methods which can be used by any laboratory, IPST is modifying its

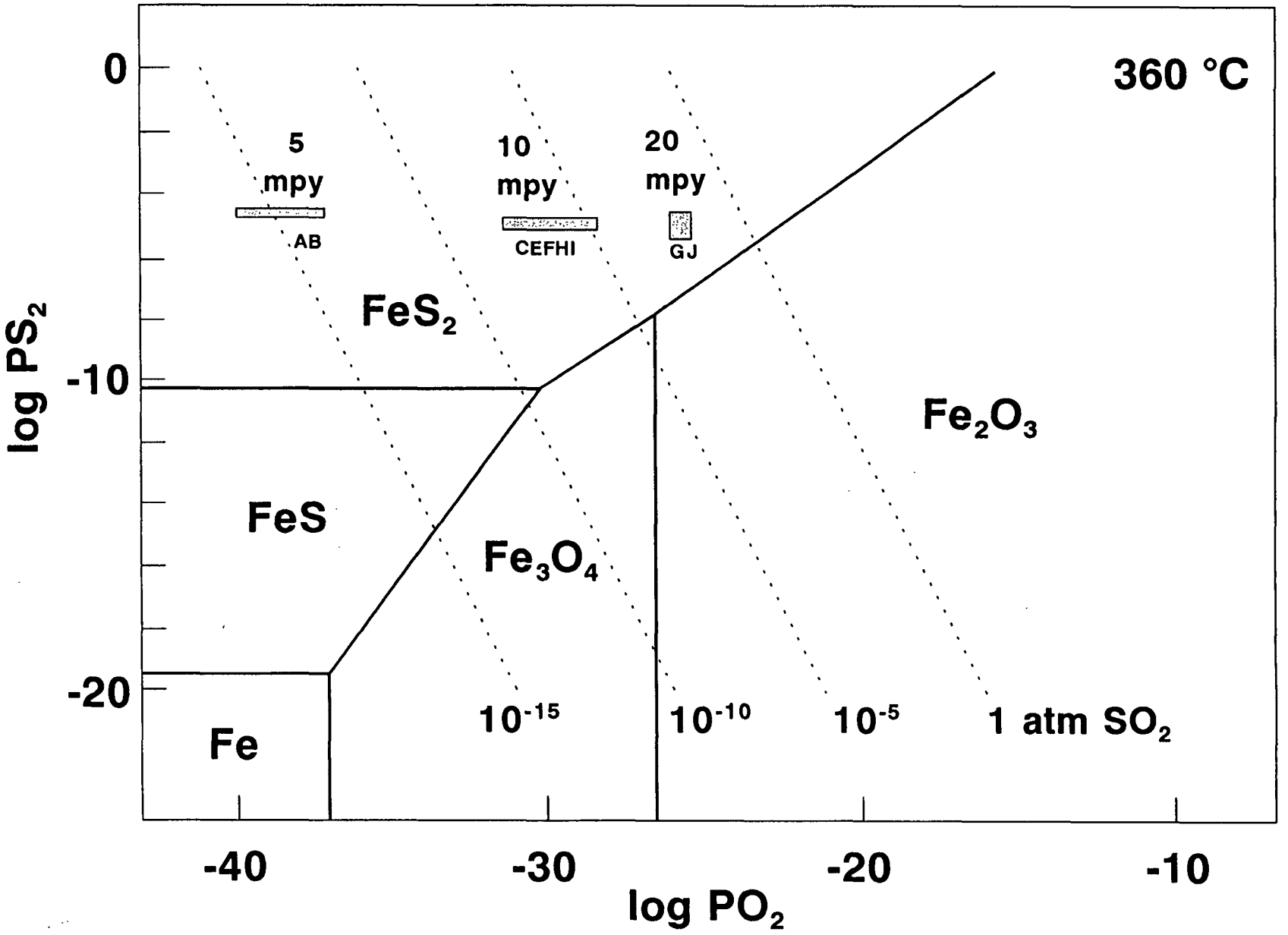

Fig. 5. Plot of Corrosion Rate Zones on Phase Stability Diagram

experimental apparatus now in an effort to match these procedures and variants for the future. The new tests are conducted in a vertical tube furnace in a simple gas environment of H_2S and N_2. Furthermore, our previous work was conducted at temperatures of 330 and 440°C, but the AFPA tests are generally run at 320 and 360°C. Also, instead of flat coupons, full-wall coupons from waterwall tubes are now used; and, burnishing is the standard surface preparation technique as opposed to grinding. Consequently, we have modified our equipment and procedures now so that future data will be useful to those interested in following the AFPA test procedures.

Experimental Setup

The single-zone tube furnace (ATS Model 3110) was attached to a uni-strut frame in order to position it vertically. A 2.5 inch diameter Vycor tube was used as the test chamber. A lower sealing cup, upper sealing flange, and flange cover plate were machined from 316L stainless steel. A hole was drilled and tapped in the sealing cup for a compression fitting which was used for the gas inlet. An O-ring was employed to seal the upper flange cover plate to the upper flange. The lower sealing cup and upper sealing flange were attached to the Vycor tube with type 732 RTV sealant. The entire furnace assembly is used in a fume hood.

Several holes were drilled and tapped in the flange cover plate for a gas outlet, a thermocouple, and a glass rod. The glass rod is used as the test coupon holder. Four 2 mm diameter Pyrex rods 1 inch long were fused perpendicularly to a 6 mm diameter Pyrex rod approximately 18 inches long. The top of this holder assembly was passed through a Cajon o-ring fitting which can be tightened to provide a gas-tight seal against the Pyrex rod and hold it at any desired level in the furnace. A schematic of the furnace is shown in Figure 6.

In the past we have used rotameters to control the relative amounts of gases entering the furnace. However, we now have two mass flow controllers which should provide very accurate flow control over the longest term experiments. MKS 100 Series Model 1159B mass

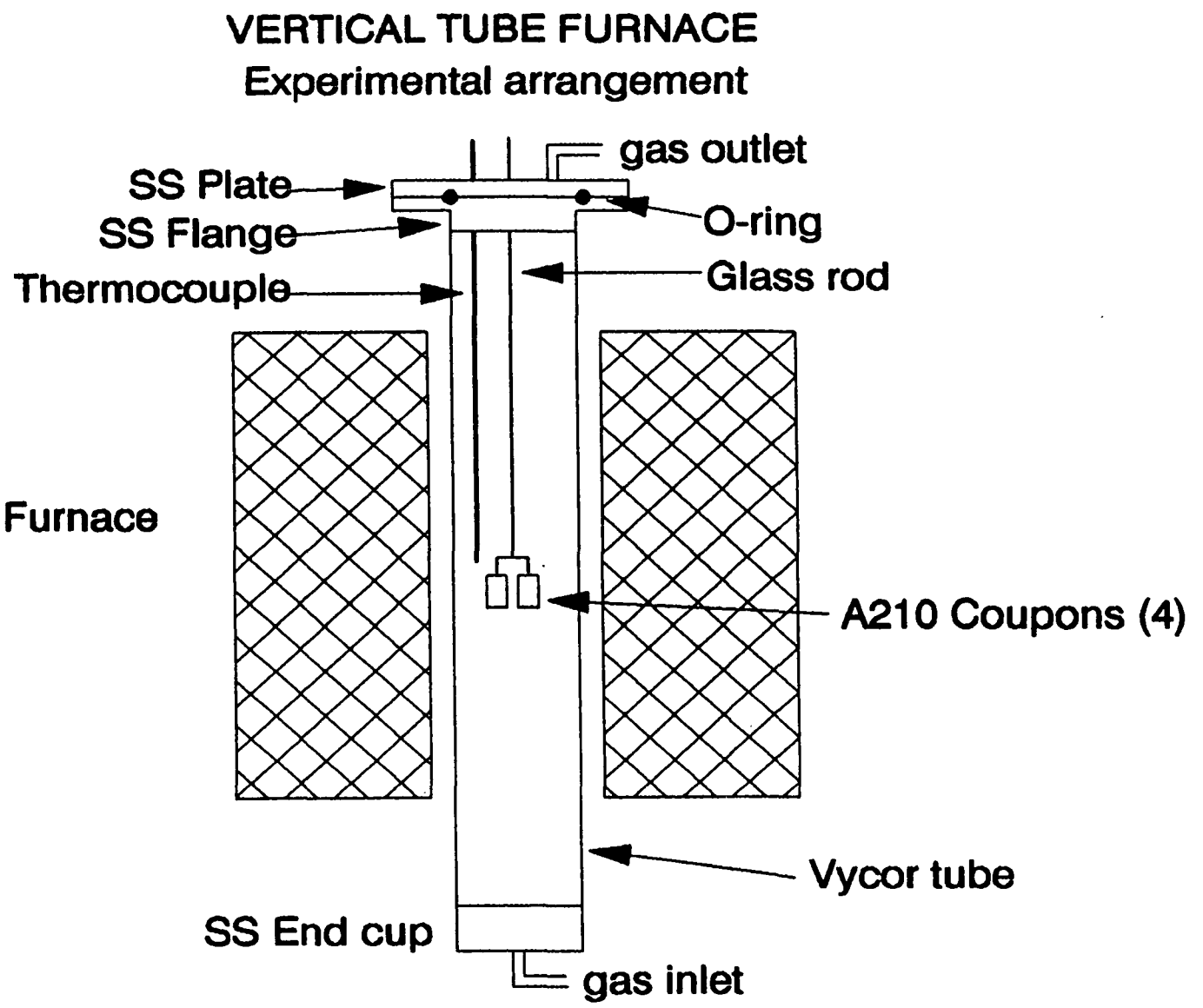

Fig. 6. Schematic of Vertical Furnace

flow controllers with an MKS Type 247C 4 channel readout are used. These controllers are calibrated for N_2, but because of the low levels of H_2S present, the calibration is still valid.

The H_2S concentrations of the gas mixtures used in these experiments were 0.1 and 1.0%. In order to reduce the number of gas cylinders required, 1.0% and 6.0% H_2S in Ultra-High Purity (UHP) N_2 were purchased. 100% UHP N_2 was used to make up the balance. Since much more 100% N_2 was required relative to the H_2S mixture, a manifold for two cylinders was used. A schematic of the entire setup is shown in Figure 7.

Procedures

Test coupons of SA-210 were purchased from Metal Samples (Munford, AL). SA-210 is now the most commonly used alloy today and has replaced the use of SA-192 in most applications. The coupons were cut from 2 inch O.D. tubes with 1/4 inch wall thickness. The size of the coupons was approximately 1"x 3/4". Upon receipt, a small hole was drilled through the wall at one end of the coupon so they could be attached to the specimen holder. A small rock tumbler (Thumbler's Tumbler Model A-R6) containing 45° triangular coarse cut ceramic tumbling and vibratory media (McMaster-Carr #4918A29) was used to provide the desired burnished surface finish to the coupons. Approximately half the coupons at a time were placed in the tumbler for 24 hours, removed to have any sharp edges smoothed with 120 grit sandpaper, and returned to the tumbler for an additional 24 hours. The coupons were then removed from the tumbler, cleaned by rinsing with acetone, and then stored in a desiccator until needed.

Before starting the tests a temperature profile of the furnace was made to determine the extent of the constant temperature zone and to determine the furnace setpoint needed to give the desired temperature inside the reaction tube. The profile was made using a NIST traceable calibrated thermocouple. The results are shown in Figure 8. As can be seen, at both of the test temperatures a constant temperature zone between 3 and 4 inches was found.

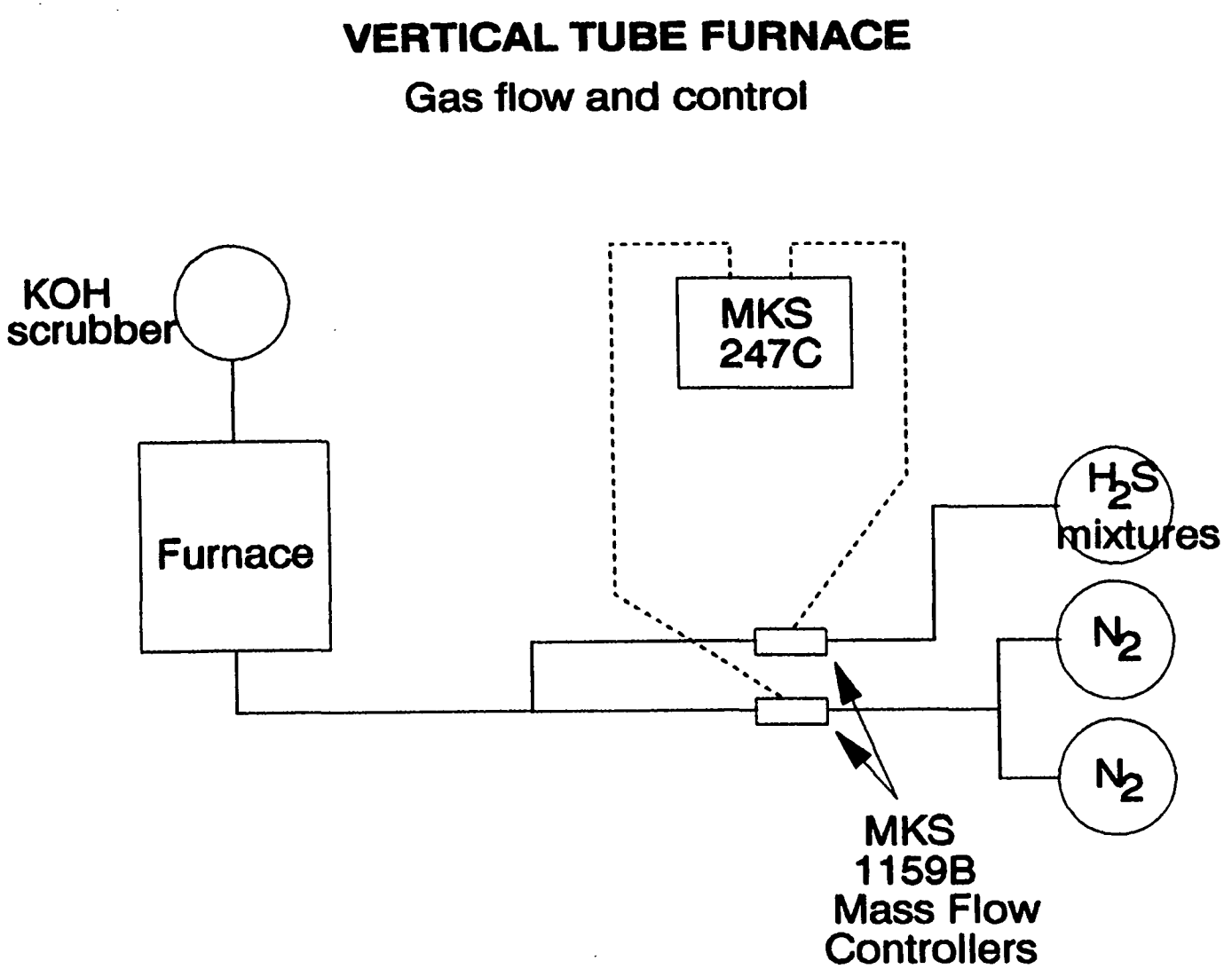

Fig. 7. Schematic of Overall Experimental Set-Up

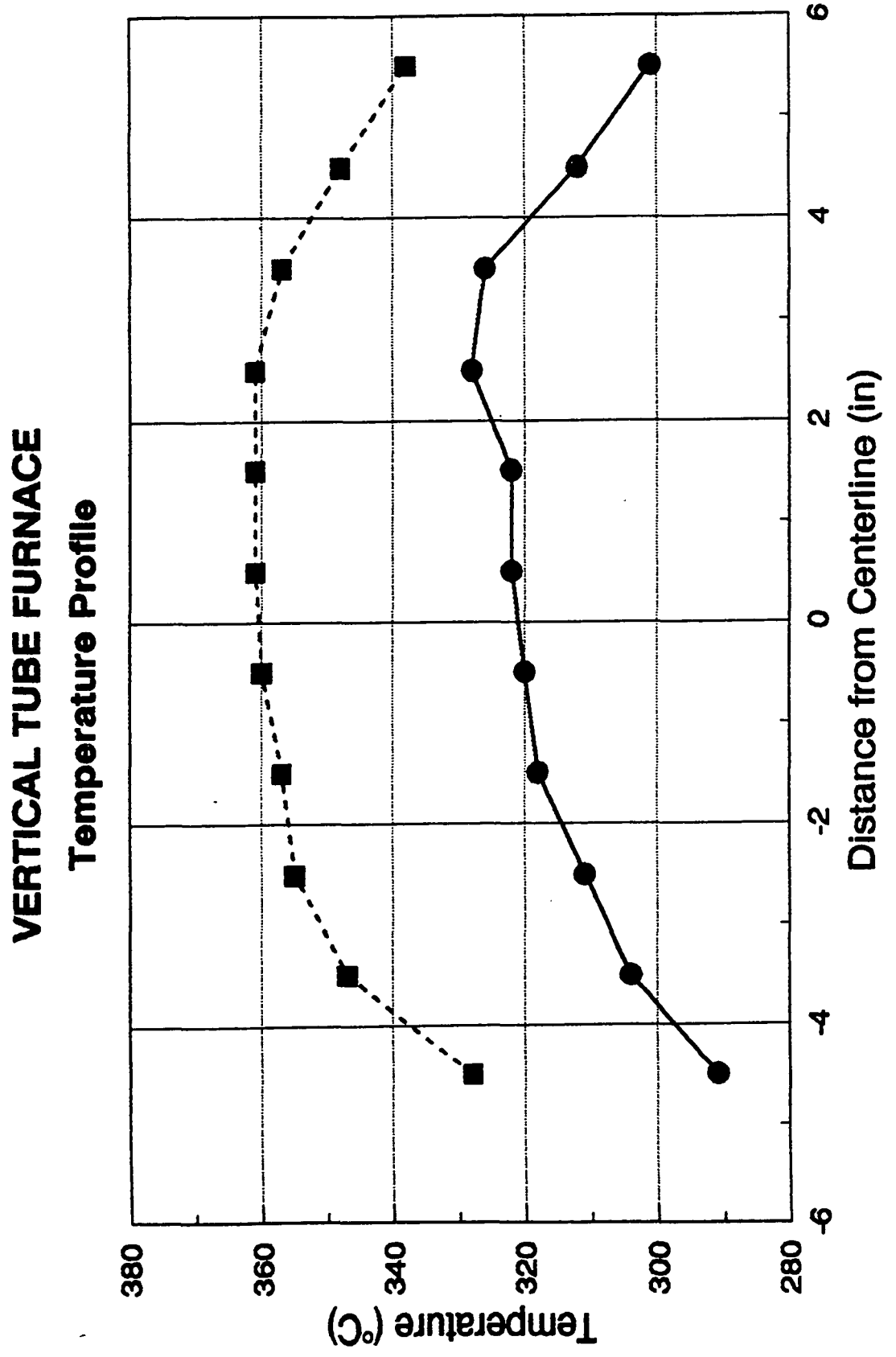

Fig. 8. Temperature Profile for Vertical Furnace

Prior to the initial test, the furnace was sealed and the temperature raised to 800°C, held there for several hours, and then allowed to cool to 100°C. After this initial soak, the following procedure was followed to ensure consistent results:

1. remove 4 coupons from desiccator and clean with acetone
2. weigh and record coupon ID and weight
3. remove upper flange plate from furnace tube
4. attach coupons to specimen holder using platinum wire
5. attach upper flange plate to furnace tubes
6. purge tube with N_2 for 10-15 minutes
7. raise furnace temperature to operating value while maintaining N_2 purge
8. turn off N_2 purge when operating temperature is reached
9. adjust gas flow to the desired level
10. record start time of test

During the course of the test the operating parameters were monitored and adjusted if necessary. A consistent procedure was also followed at the end of every test, and included cooling the specimens overnight in flowing nitrogen. After removal from the furnace the specimens were visually inspected and stored in a desiccator until ready for metallographic preparation or weight loss determination. The specimens used for corrosion rate determination were cleaned by blasting with glass beads, and then rinsed with acetone. Calibration coupons have been tested to ensure that significant unreacted metal is not removed during glass bead blasting.

Results

The first series of tests was conducted to reproduce the AFPA standard test and compare our results with those obtained by the Pulp and Paper Research Institute of Canada (PPRIC). The visual examination of all test coupons showed that there was very little, if any, difference in

appearance among coupons exposed during the same test, or in the different tests for that matter. All of the coupons had a dark gray sooty outer corrosion layer for the tests conducted in this sulfidizing atmosphere. There was no cracking or spalling observable on any of the test coupons.

A summary of the weight loss results is given in Table 3 along with a comparison with the results from PPRIC. The corrosion rate for all tests was fairly low and both coupons in each test were very similar. Unfortunately, only the maximum corrosion rate was recorded for several of the PPRIC tests so a direct comparison is difficult to make. PPRIC used a chemical cleaning method as opposed to our glass bead blast, and they used more coupons, so perhaps that could account for the differences.

Coupons were also exposed to the UHP nitrogen atmosphere for 5 days to determine baseline conditions. Only a thin tarnish film was present and the rates were less than or equal to 1 mpy. These experiments were conducted for half the exposure period compared to the H_2S tests, and it would be expected that the rates would be lower over a 10 day period

Metallographic examination of the scale revealed that it was composed of two layers. The outer layer had the columnar appearance typical of an iron sulfide layer with many breaks and pores. The inner layer was very dense and no breaks or cracks were apparent. The outer layer was about twice as thick as the inner layer with a total scale thickness of 4-10 microns.

Table 3. Summary and Comparison of AFPA Standard Test Results

Gas	Temperature	Time	Corrosion Rate(IPST)	Corrosion Rate(PPRIC)
UHP N_2	360°C	5 days	1.0 mpy	
UHP N_2	320°C	5 days	< 1 mpy	
0.1% H_2S	360°C	20 days	2.5 mpy	8 mpy (max)*
0.1% H_2S	320°C	10 days	2.1 mpy	4 mpy (max)
1.0% H_2S	360°C	10 days	4.4 mpy	7 mpy (max)
1.0% H_2S	320°C	10 days	5.4 mpy	4.4 mpy

*PPRIC result is for 10 days

Task 2. Local S and O Activities

The local thermodynamic conditions beneath a frozen smelt layer will obviously control the kinetics of scale growth more than the bulk gas chemistry in the furnace. While it may be possible to develop models to predict these conditions, it is always better if a direct measurement can be made.

The objective of this task is to develop a technique based on solid electrolytes. Solid electrolytes are typically exclusive ionic conductors which can be used to measure a thermodynamic quantity, relative to the conducting species, on one side of the electrolyte if the value on the other side is known. Thus, if that value is fixed in an experiment, the device becomes a probe capable of determining instantaneous values for the thermodynamic potential of interest. For this case, we are primarily interested in knowing what the local sulfur and oxygen activities are beneath the smelt, because these conditions will control sulfidation and oxidation kinetics.

During last year's report, the use of sulfate electrolytes for measuring S_2 and O_2 partial pressures as a product was discussed. However, it was pointed out that to obtain the absolute value for the sulfur partial pressure from such a measurement, an oxygen probe would also be needed for an independent measurement of oxygen partial pressure. The results reported at that time were concerned with determining whether a standard zirconia oxygen gauge could be used for this purpose. It was found that at the temperatures of interest for kraft recovery boiler waterwall tubes zirconia will not function as an exclusive oxide ion conductor. Efforts during the past year were made to determine if modifications to the standard zirconia cells had ever been reported which would make them useful at lower temperatures. Unfortunately, no information was found which would allow the use of oxygen measurements to further the development of the sulfur cell.

As a result of these findings, it was decided to consider whether the output of the sulfate based sulfur-oxygen sensor could be of some use in predicting the onset of rapid sulfidation conditions relative to the normally benign oxidation condition.

The electrochemical cell makes use of sodium sulfate as a sodium ion conductor. A schematic of the arrangement is given in Figure 9. The emf of the cell is given by the following equation:

$$E = \frac{RT}{F} \ln \frac{P'_{Na}}{P''_{Na}}$$

which can also be expressed using the SO_2 and O_2 pressures,

$$E = \frac{RT}{2F} \ln \frac{(PSO_2PO_2)'}{(PSO_2PO_2)''}$$

Thus, the sulfur and oxygen activities cannot be determined independently. Given the difficulty of trying to measure oxygen using another type of sensor, so that sulfur can be calculated, an attempt was made to consider the output of the sensor relative to the phase stabilities in the Fe-S-O system. The rationale for this approach was that the sensitivity of the sensor may allow approximations of phase stabilities to be made, since the presence of iron sulfides, as opposed to iron oxides, appears to initiate rapid corrosion kinetics in recovery boilers with carbon steel waterwalls.

Figure 10 shows the Fe-S-O phase stability diagram at 360 °C. Superimposed on this diagram are lines of constant SO_2 as well as lines of constant voltage from the sulfate sensor. It was assumed that the reference side of the sensor would be fixed by the equilibrium between $Fe/FeS/Fe_3O_4$ to calculate these voltages. It can be seen that for a given emf from the cell, a wide variety of sulfur and oxygen activities are possible, so it would not be

Sulfur Sensor

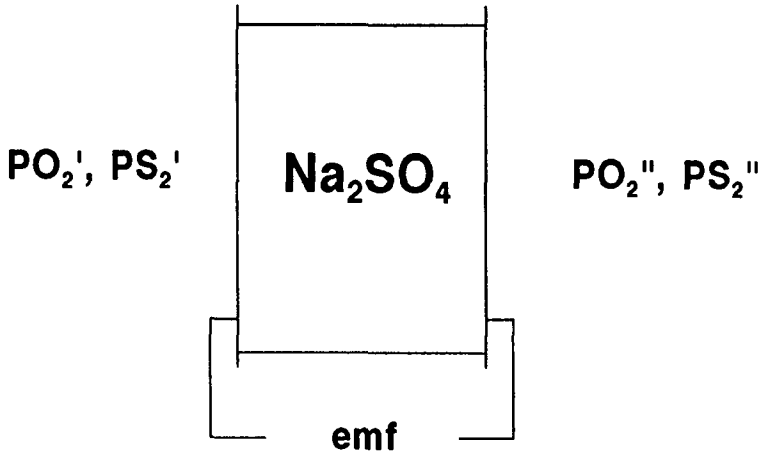

$$emf = \frac{RT}{4F} \ln \frac{PS_2' \, PO_2'^4}{PS_2'' \, PO_2''^4}$$

$$emf = \frac{RT}{2F} \ln \frac{(PSO_2 \cdot PO_2)'}{(PSO_2 \cdot PO_2)''}$$

- **Need Independent Measure of Oxygen or Sulfur**

Fig. 9. Schematic of Sulfate Sensor

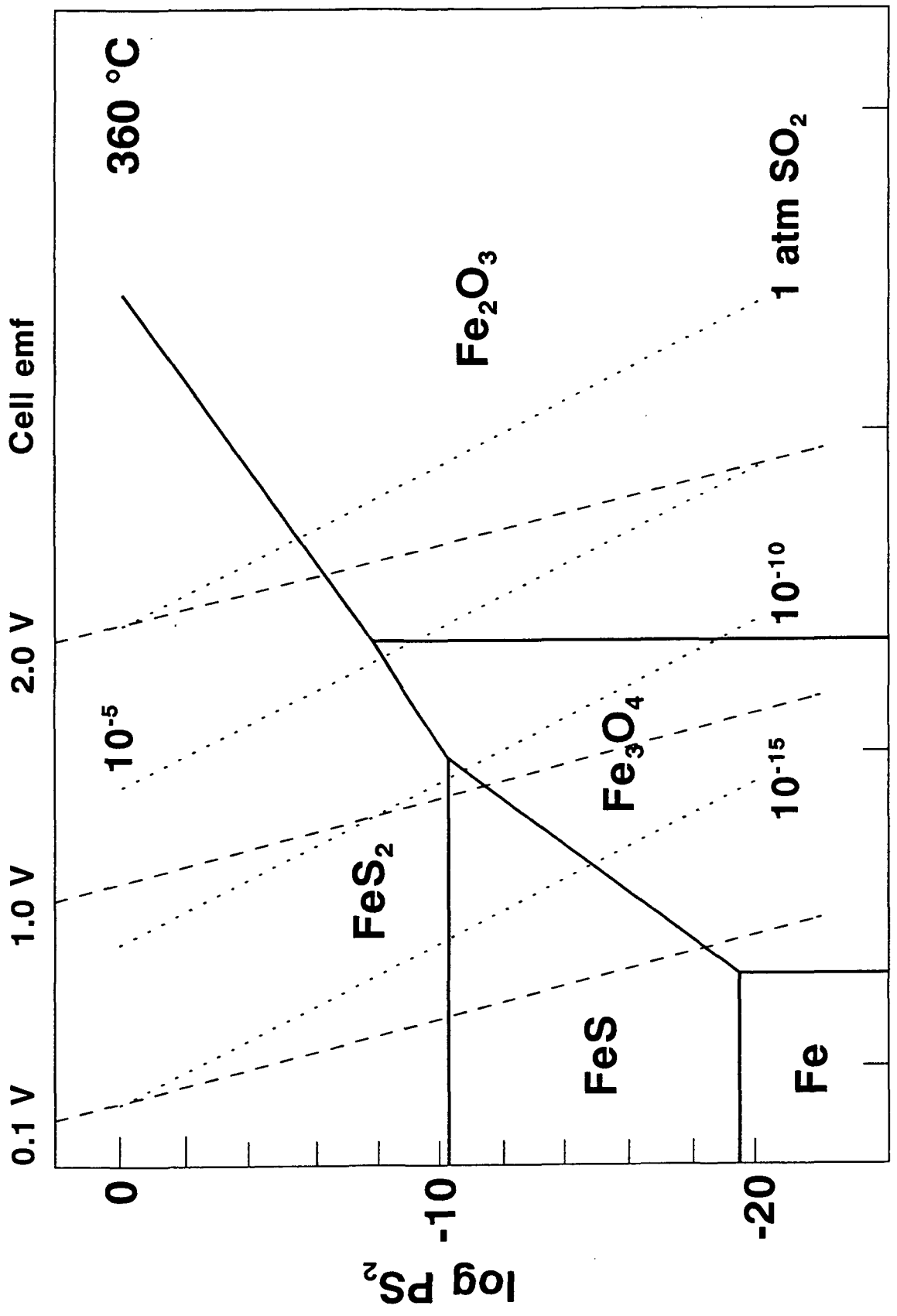

Fig. 10. Constant Voltage Output Lines for Sulfate Sensor. For Fe/FeS/Fe_3O_4 Reference.

possible to estimate if the local environment beneath smelt is in a stable oxide or sulfide field for iron.

As an alternative, another approach to determining the position along the constant voltage output line has been developed. Rather than trying to measure oxygen independently, an approach to measure sulfur over a limited range may also be possible and useful. There are reports that a AgI solid electrolyte can be successfully used as a sulfur sensor. Figure 11 gives the results from one study which gives temperature and sulfur pressure bounds. The cell is given by the following:

$$\mathbf{Pt, Ag} \;\|\; \mathbf{AgI} \;\|\; \mathbf{Ag_2S, S_2, Pt}$$

For the cell to be an accurate sulfur sensor, it has been reported that no oxygen be present because the Ag_2S reacts to form SO_2, which would consume part of one component of the cell. However, in the low oxygen pressures required for iron sulfides to be stable on carbon steel, the kinetics of such a reaction may be very slow, and the consumption of the silver sulfide may be negligible. Consequently, while this technique may have application only over a limited range of sulfur pressures, this may be in the range of interest for kraft recovery boilers. Another potential problem is that the cell will only function where silver sulfide is stable, the lower limit of which is about midway between Fe/FeS and FeS/FeS_2 at 360 °C. Consequently, the sensor would only work at the more elevated values of sulfur partial pressures; this may not be a problem because the output might be subsequently linked to areas of severe corrosion rates and could thus function as a go/no-go type of sensor when coupled to the sulfate sensor.

Thus, it appears that this technique has merit and warrants further study, given the importance of the information which may be obtained.

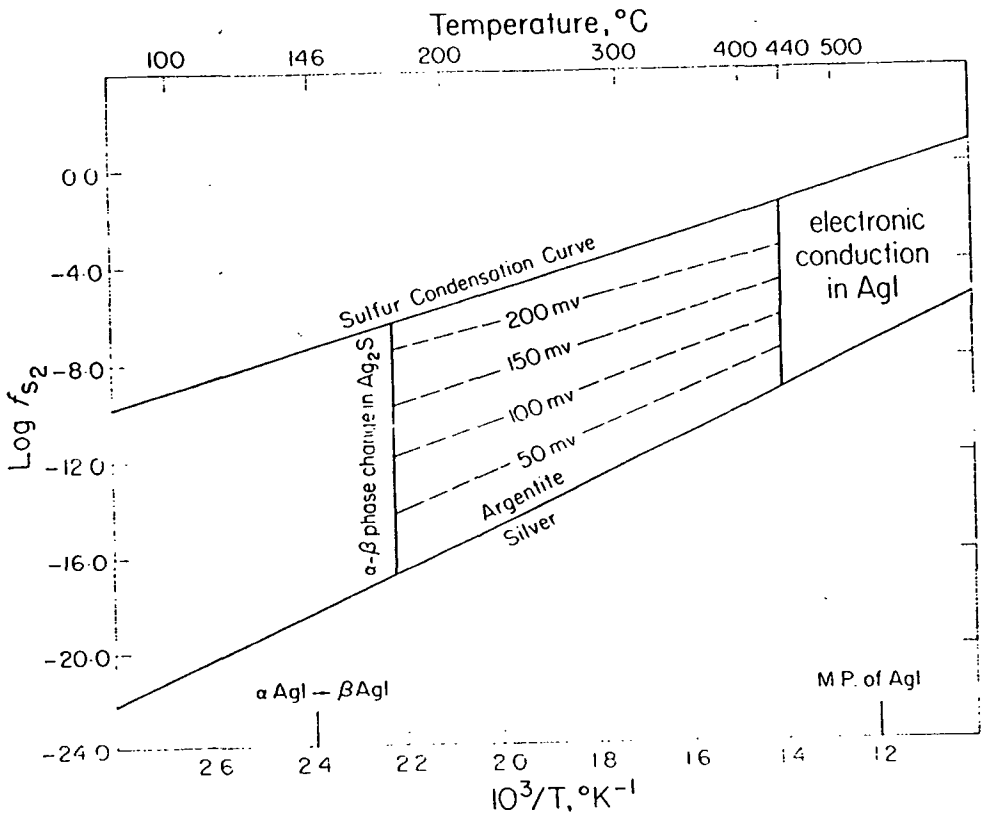

Fig. 11. Range of Sulfur Partial Pressures Measurable with AgI Cell. After Schneeberg, Econ. Geol. 68, 507, (1973)

Task 3. Long-term Kinetics

Boilers are designed to operate for many thousands of hours without replacing waterwall tubes. Indeed, even between scheduled shut-downs, the boiler must operate for 4,000 to 8,000 hours, depending upon the interval. Most of our laboratory tests are at most a few hundred hours and usually much less than that. From the laboratory data, an estimate of remaining life is made based on these short-term kinetic experiments, and alloy rankings result. An implicit assumption in this approach is that the kinetics do not change and the rate laws developed are constant. This has not been demonstrated for this application, and our data generated by discrete weight change measurements indicate gaps which need to be better defined if accurate kinetic rate laws are to result. In other industries a phenomenon known as breakaway corrosion has been reported for stainless steels. Breakaway corrosion occurs as a result of depletion of the scale-forming element and causes the kinetics to change from parabolic to linear with a higher rate constant. This task is designed to determine whether this phenomenon is likely to occur in the recovery boiler environment by making continuous measurements of the weight change.

Experimental Procedures

The previous technique for establishing kinetics has been by determining weight loss of an individual coupon after a specific time of exposure. A summary of this approach is given by the data shown in Figure 12. As can be seen, the intermediate kinetics will control the long-term behavior. Consequently, in this task a different approach will be used. A continuously recording thermobalance will allow the weight of the specimen to be recorded so that any changes in the rate constant will be immediately apparent.

The experimental setup is shown in Figure 13. The balance was placed on top of a frame which holds a vertical tube furnace. A platinum wire was used to support the test specimen from the balance and is adjusted so that the specimen is located at the furnace hot zone. Gas

Weight Loss Kinetics

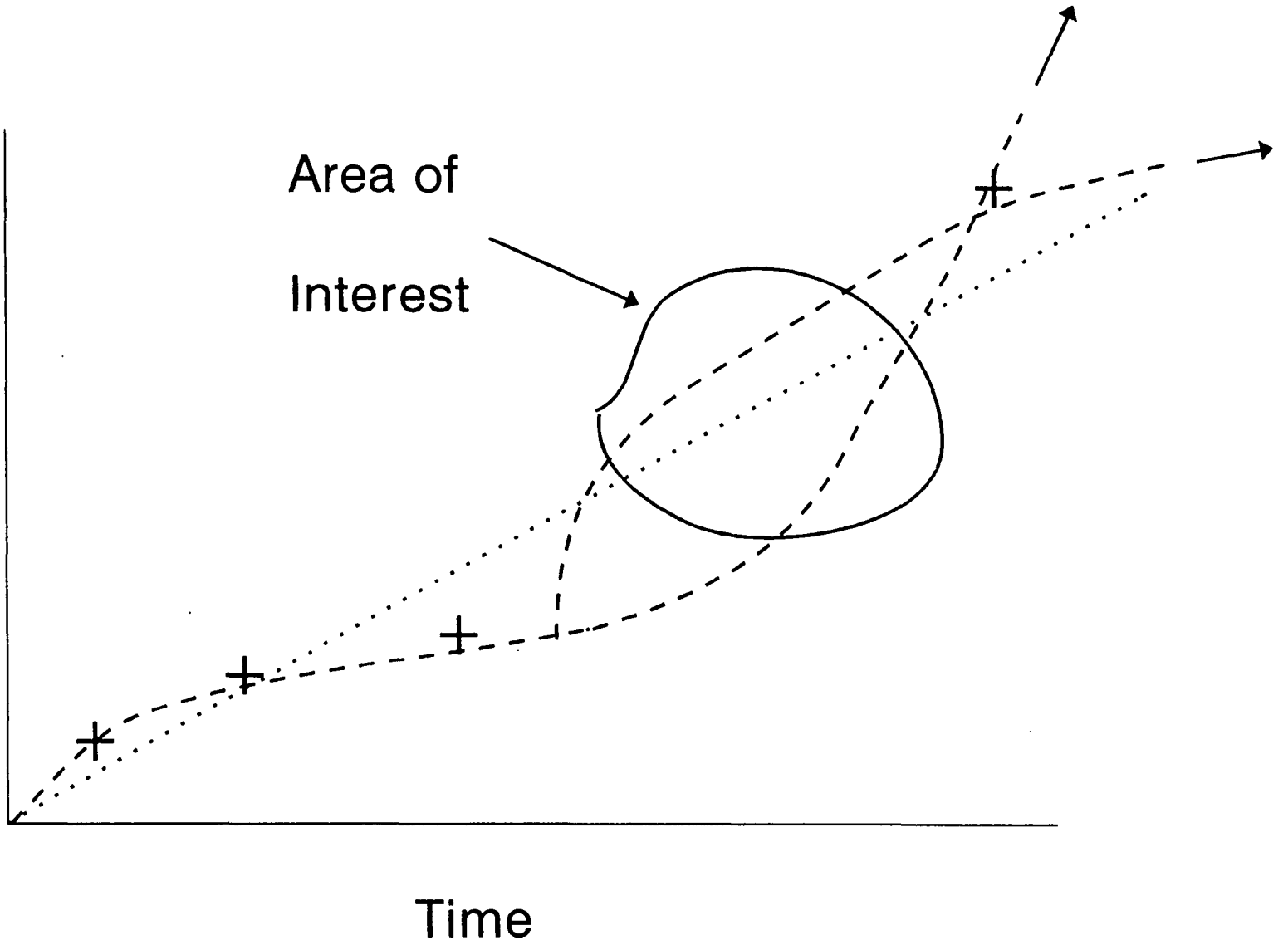

Fig. 12. Weight Loss vs. Time for Different Kinetic Rate Laws

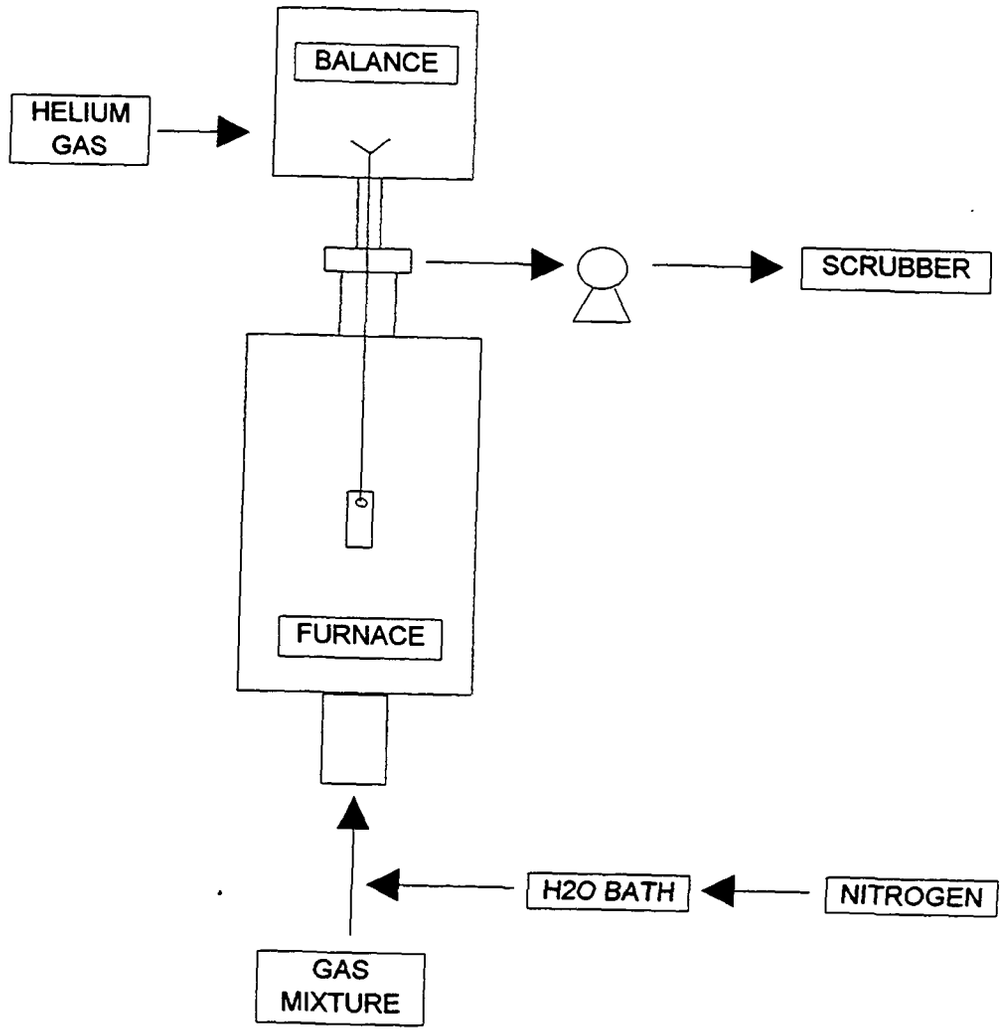

Fig. 13. Schematic of Experimental Set-Up for TGA Runs

is admitted into the furnace through the bottom and exits above the furnace but below the balance. Provisions for an inert gas purge of the balance were made to protect the balance from hydrogen sulfide while allowing any unwanted gases to be flushed from the system. A small vacuum pump was added to the outlet line as insurance to ensure that the corrosive gas exited beneath the balance. The balance provides a voltage output which is recorded on a strip chart.

Results

Work on this task was conducted by an M.S. student, Lisa McMillian, who graduated in March, 1993. The first objective of the project was to set up the balance for hydrogen sulfide, which would extend the results of the air tests reported during the last period. The next objective was to develop the kinetic curves for carbon steel in environments which were located in oxide and sulfide fields on the phase stability diagram. Moreover, the effect of instantaneous changes from oxidizing to sulfidizing were also to be examined. The targeted environments are shown in Figure 14.

Initial experiments resulted in plugging of the gas outlet line, so the apparatus had to be modified to enlarge the diameter of the outlet line. Once this problem was solved the experiments began, but at the conclusion of the first run, it was discovered that deposition of solids from the gas had occurred on the hang-down wire. From a separate overall weight change measurement, it was determined that the deposition was close in magnitude to the change in the weight of the coupon, which made data analysis impossible. The apparatus was then modified to provide heat tracing at the top of the furnace in an attempt to move the deposition point outside the furnace where it would not have an impact on the measurements. This was not successful in eliminating the deposits, so the temperature was obviously not hot enough, but in any case the o-ring seals were hardened at this point, so a major redesign would be necessary to continue with this approach.

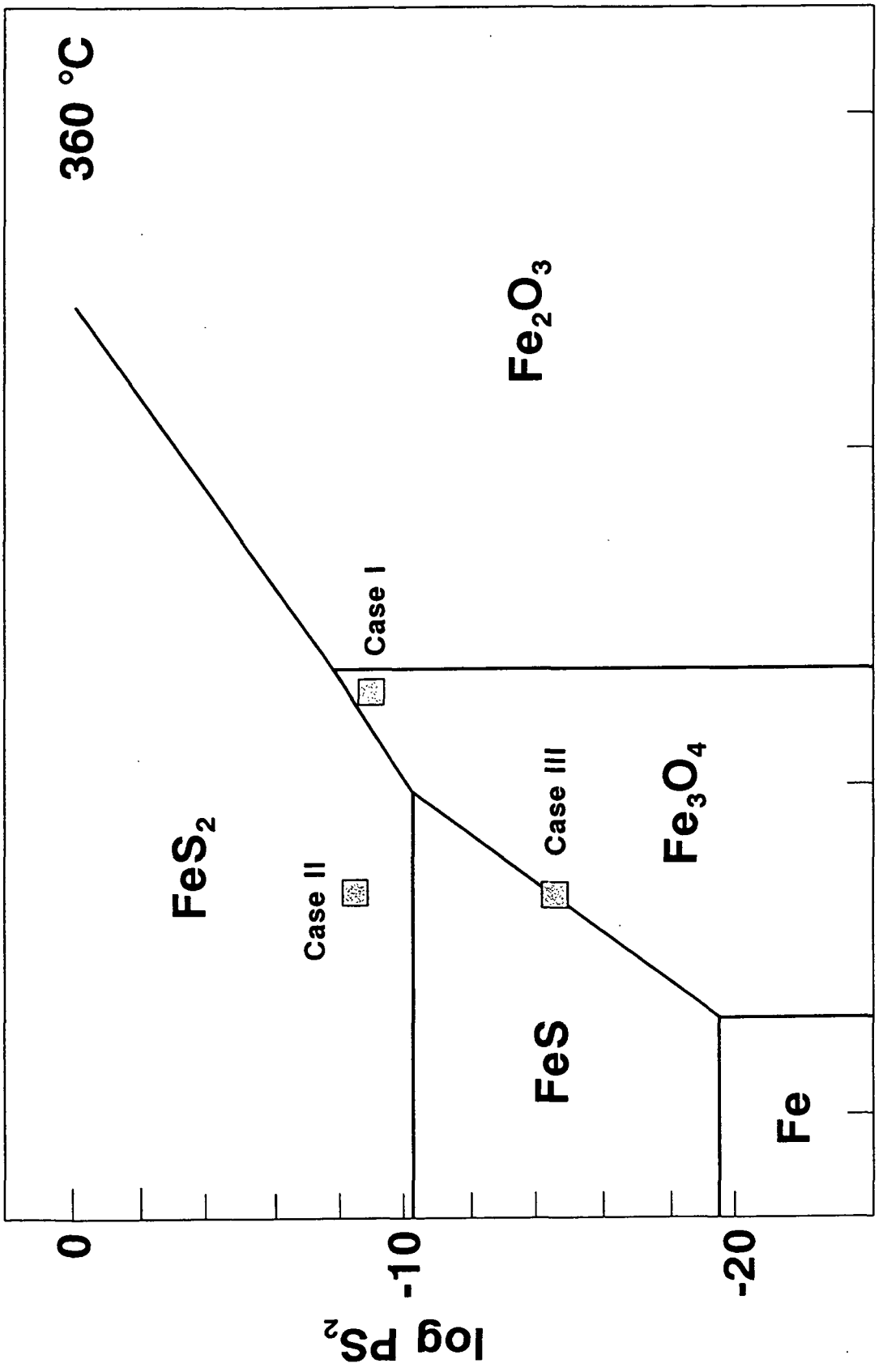

Fig. 14. Plot of Experimental Conditions for Preoxidation Tests on Phase Stability Diagram

Another approach was taken to reverse the gas flow to make the inlet at the top and the outlet at the bottom of the furnace. If the deposits were caused by heating and then cooling the gas, the flow reversal should have stopped deposition. The apparatus was changed, but the deposition continued. Additional problems surfaced after a number of these trials, and were traced to hydrogen sulfide getting past the helium purge gas and damaging the balance. At this point the continuous kinetics objective of the project was abandoned and a shift to a morphological study was made, where changes from oxidizing to sulfidizing conditions were examined.

The modified study was conducted to determine the effects of preoxidation on subsequent sulfidation. Specimens of carbon steel were oxidized in the stable oxide field for 2 days (Cases I and III of Figure 14) and then the gas was changed to Case II for 5 days. Comparisons with 2-day exposures in the Case I and Case III environments exclusively were then compared. SEM examination revealed that preoxidation under Case I conditions rather than Case III conditions yielded a thinner sulfide scale when the gas mixture was changed to Case I. Baseline oxidation conditions without sulfidation only produced very thin scales which were barely resolvable using the SEM. Consequently, no remnants of the oxide scale could be seen beneath the sulfide scale for those tests that were initially oxidizing and then sulfidizing. If the oxide scale had been thicker, then clues about the scale breakdown mechanism might have been available.

As a result of this work, it is apparent that there are experimental difficulties in making continuous kinetics measurements in the environments of interest for recovery boilers. The probable reason for this is the presence of water vapor, so if a simplified gas without water could be used, this problem likely may be alleviated. However, it is also likely that a gas of this composition would not be oxidizing to iron, which was the intent of part of this task. We have a few ideas about modifications to the apparatus which may minimize the deposition problem, but these will require some time and expense to evaluate. Consequently, this effort will not receive high priority in the near-term, unless another M.S. student shows an interest.

Task 4. Air Port Corrosion

In the last report a theory was proposed to explain the phenomenon of air port corrosion of composite tube boilers. An essential element of the theory is that stable oxides present on the alloys are subject to accelerated dissolution in a molten salt because of oxidation-reduction reactions. The variation of oxide solubility through the salt is also a key element, and the oxide solubility varies with melt basicity. There is strong indication from field measurements that the molten salt is NaOH-based. Consequently, both stainless steel and carbon steel were laboratory tested in molten NaOH to determine the corrosion rates. Experiments conducted for the last report showed that the melt basicity had an influence on corrosion, but the actual value of basicity is unknown because a probe still needs to be developed.

The corrosion rates of carbon steel, stainless steel and nickel are summarized in Table 4. The new data for nickel is given along with the previous data for carbon steel and stainless steel. The data was generated for three different basicities: the normal melt using dry air as a cover gas, the basic melt made by adding Na_2O_2 and the acid melt made by increasing the water vapor content of the gas.

While the actual basicities of these melts are not known, we can plot the corrosion rates for each of the three alloys at the three basicities on an arbitrary basicity axis. Figure 15 is a plot of corrosion rate (mg/cm^2 for 72 hours) versus basicity, using an arbitrary scale for basicity. The dashed lines are visual estimates and show how the transition from acid dissolution to basic dissolution might occur. The only point to be made is that the corrosion rate curves tend to mirror the oxide solubility curves found in other molten salt systems, and thus support our approach to measure the oxide solubilities in this system.

Table 4. Effect of Basicity on the Corrosion of Carbon Steel, Stainless Steel, and Nickel in NaOH at 320°C for 72 hours. Cover Gas is Dry Air Except for the Water Vapor Case.

	Weight loss (mg/cm^2)		
Environment	C1010	304 SS	Nickel
NaOH + 10% Na_2O_2 (basic)	25.7	43.2	0.3
NaOH	13.2	26.2	0.9
NaOH + 80% H_2O(g) (acidic)	145.7	10.4	3.9

Effect of Basicity on Corrosion

NaOH at 320 C for 72 hrs

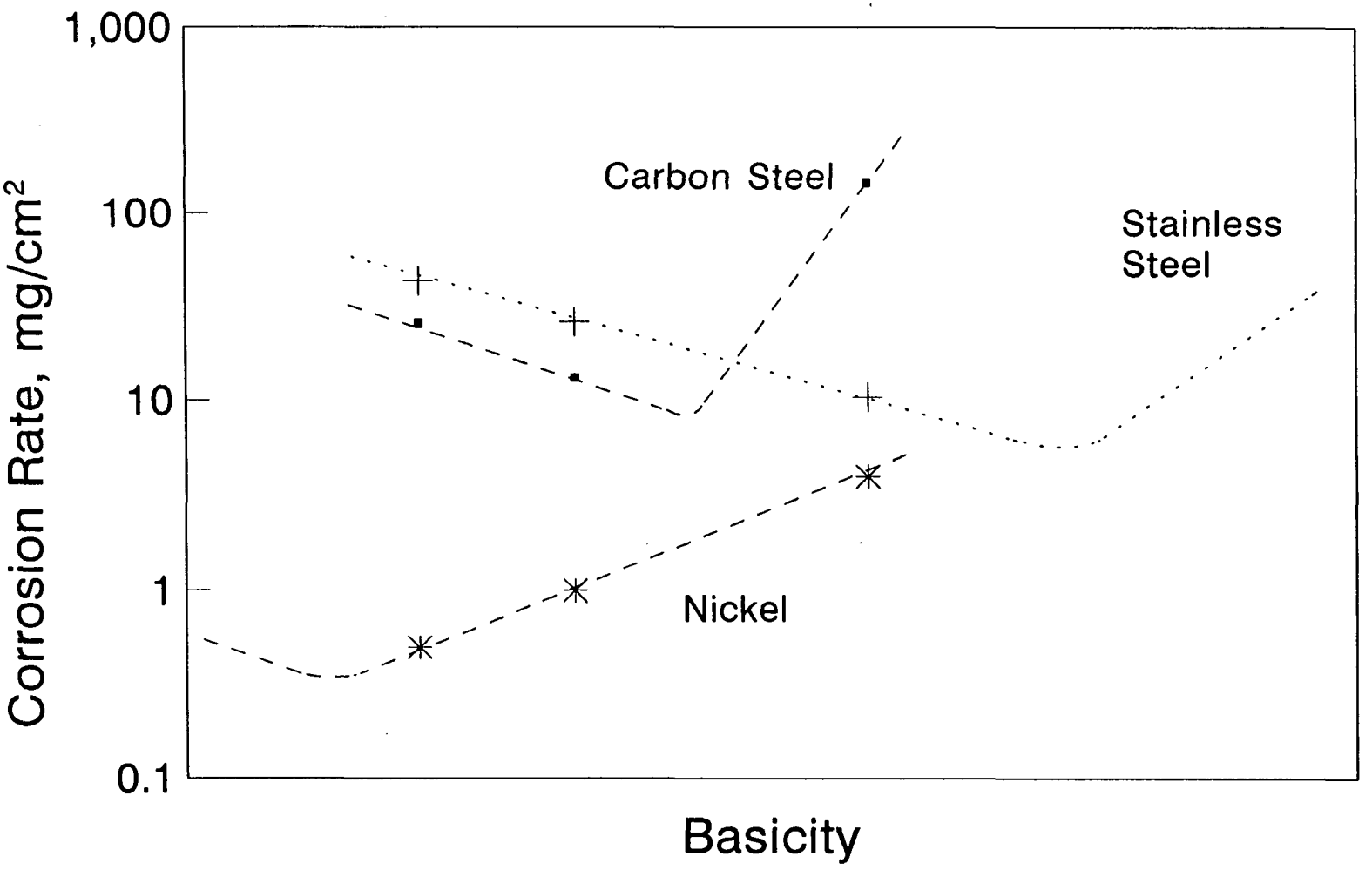

Fig. 15. Effect of Basicity on Corrosion Of Carbon Steel, Stainless Steel and Nickel in Molten NaOH

Oxide Solubilities

The physical test arrangement was the same one that was used for measuring weight loss (Figure 16). A vertical tube furnace with a removable stainless steel retort and a high purity alumina crucible were used to comprise the test chamber and molten NaOH container. The desired test gas was fed into the test chamber through a stainless steel tube which terminated near the top of the ceramic crucible. The gas was exhausted through another stainless steel tube opening near the top of the retort to prevent short circuiting the gas.

The sodium hydroxide used is supplied in pellet form, which is then ground into a powder using a mortar and pestle so that more NaOH can be placed in the crucible. The NaOH powder was poured into the crucible until it was about 1/3 full. About 1 gram of powdered metal oxide was then added to the crucible, and then it was filled to the top with NaOH. There were approximately 20 g of NaOH in the crucible.

After the charged crucible was placed in the furnace, the gas flow was started and the test chamber brought to 320°C.

Periodically samples of the NaOH melt were taken. This was accomplished by removing the plug from the rubber stopper and inserting a ceramic rod into the melt. The ceramic is quickly and carefully inserted into the surface of the melt in order to have the salt freeze to the rod, but, ideally, not inserted so far that the undissolved metal oxide powder is also taken. In the case of Cr_2O_3 this was apparent because the oxide powder is green while the melt is bright yellow color of chromate. The rod was removed from the test chamber and the plug reinserted.

The frozen smelt sample was dissolved into 10 ml of water in a glass vial and refrigerated until the analysis could be completed. The sampling procedure was repeated several times to try to reach an equilibrium value, or until the remaining melt volume was too small to obtain

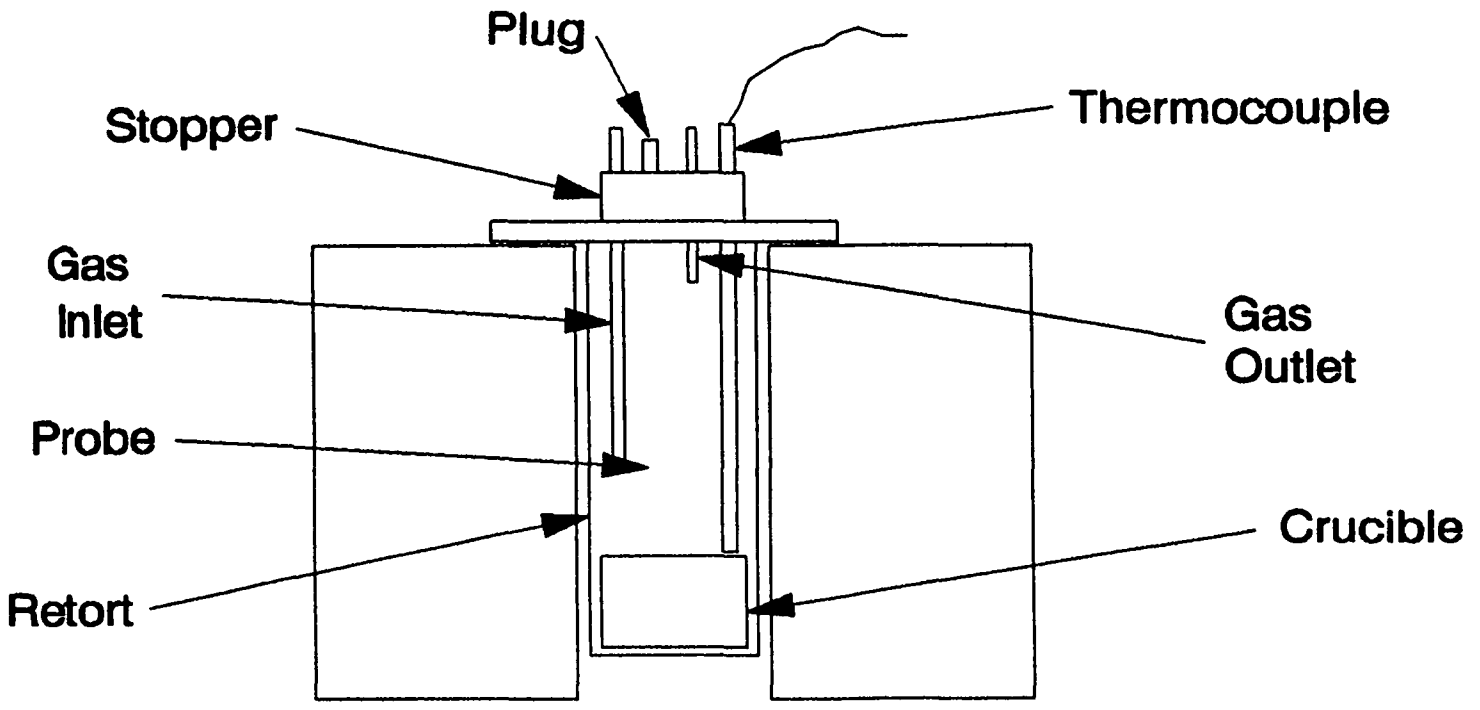

Fig. 16. Experimental Arrangement for Oxide Solubility Studies

a sample. The samples were analyzed for the metal in the metal oxide, and for chromia it was also possible to determine chromate ion concentration. The results of the analyses are shown in Table 5 and in Figure 17.

As can be seen from the table and graph the direct chromium measurement and the indirect chromate measurement compare very well at the two points where both were made. As can be seen from the graph, the sixth data point shows a break in the curve, which would be expected if the solubility had been reached. Subsequent data points show an ever increasing amount of Cr in solution, but not at the same rate, and with apparently more scatter. This is either the result of the melt volume becoming so small that samples could not be taken without Cr_2O_3, or that the solubility was not reached. A least squares fit to the first 5 data points resulted in the equation:

$$\%Cr = 0.05\ t^{0.73}$$

where t is in hours. This curve is superimposed on Figure 17, where it is extrapolated to the maximum time of our experiments. The value expected is very close to the last point measured, so it is unclear about whether the solubility was reached at 100 hours, or if it was not reached after 600 hours.

Because this initial experiment showed the need to continue this line of work and our equipment was not originally designed for such experiments, the apparatus was redesigned.

The existing tube furnace had only a 1 inch inside diameter which made it very difficult to install all the ports. Because it was desired to have some sort of probe to measure the basicity of the melt to correlate with solubility, a larger inside diameter furnace was needed. In order to reduce the costs of a new furnace it was constructed at IPST mostly using available equipment and materials. Except for the heater core and the ceramic tube all parts were available.

Table 5. Chromium (III) Oxide Solubility in Molten NaOH

Sample Weight(g)	Time (hr)	Ion conc. (mg/L)	Total Cr (mg)	% Cr direct	% Cr (as Chromate)
0.0785	24	40.6	0.406	0.517	
0.0581	48	46.5	0.465	0.800	
0.0533	97	73.6	0.736	1.341	
0.0462	120	76.2	0.762	1.649	
0.0735	170	156.3	1.563	2.127	
0.0744	216	140.4	1.404	1.887	1.847
0.0467	288	178.3	1.783	3.818	
0.0289	360	173.3	1.733	5.997	
0.0260	480	229.0	2.290	8.808	
0.0220	624	134.1	1.341	6.095	6.440

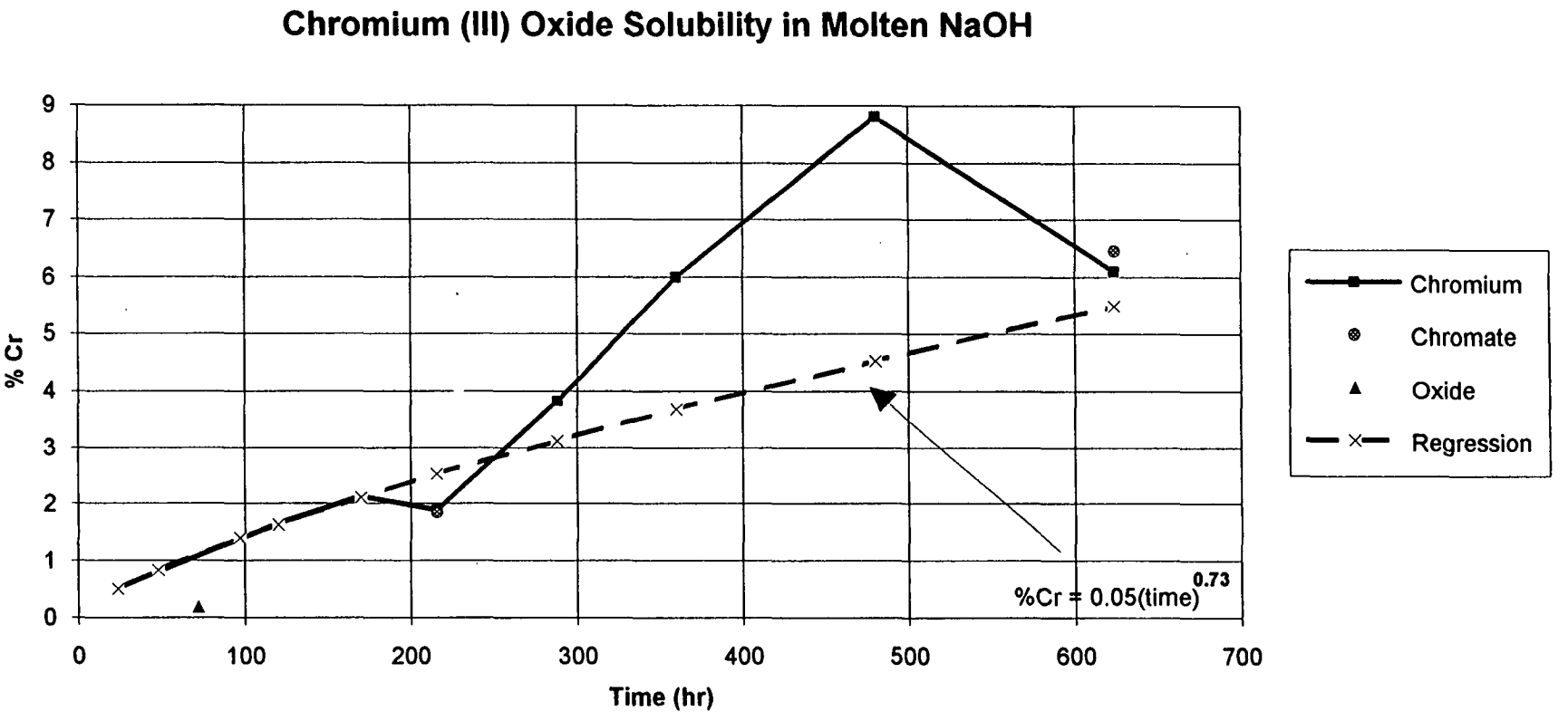

Fig. 17. Chromium Oxide Solubility Measurements vs. Time for NaOH

A schematic of the new furnace is shown in Figure 18. The heater core (Omega Engineering, Inc. #CRFC-46/240) has a 4 inch inner diameter, a 7 inch outer diameter, and is 6 inches in height. The core was centered in a stainless steel sheet formed into a cylinder 7 inches high and 9 inches in diameter. A 1/2 inch thick ceramic fiber insulating sheet was fitted to the bottom of the can before the core was inserted. The power leads were insulated with ceramic beads and passed through ceramic tubes installed in the metal can. The open space between the can and the core was filled with loose ceramic fibers for more insulation. The top of the core was covered with another 1/2 inch ceramic fiber insulating sheet that had a 4 inch hole cut in the center. A stainless steel cover plate with a 4 inch hole was bolted to the top of the furnace to complete the mechanical protection. Temperature control is provided by a unit modified to supply 208 V to the furnace.

The test chamber for this furnace was constructed using a large ceramic tube open at one end and a 316L stainless steel flange with a viton gasket to seal against the tube. An alumina disc was placed in the bottom of the tube to provide a flat surface for the crucibles. The larger diameter test chamber allows the necessary ports to be placed in the upper flange. The entire test apparatus was assembled and tested to insure that everything was working as desired. Further experiments were put on hold pending the arrival of a post-doctoral associate who would be assigned to the project full-time.

Phase Stabilities in NaOH

A thermodynamic stability diagram similar to those published by Pourbaix have been constructed for NaOH. This is given in Figure 19 where potential is plotted against the basicity parameter, -log a_{Na2O}. This is equivalent to the diagram in aqueous corrosion where the stability field for water is constructed. Figures 20 and 21 show overlays of the Fe and Cr system, respectively. The Fe diagram was constructed from theoretical and experimental data and published by Skeldon (Corrosion Science, 26, 485, 1986), and the Cr diagram was constructed at IPST from theoretical data. The accuracy of the data used for the construction

Oxide Solubility Furnace

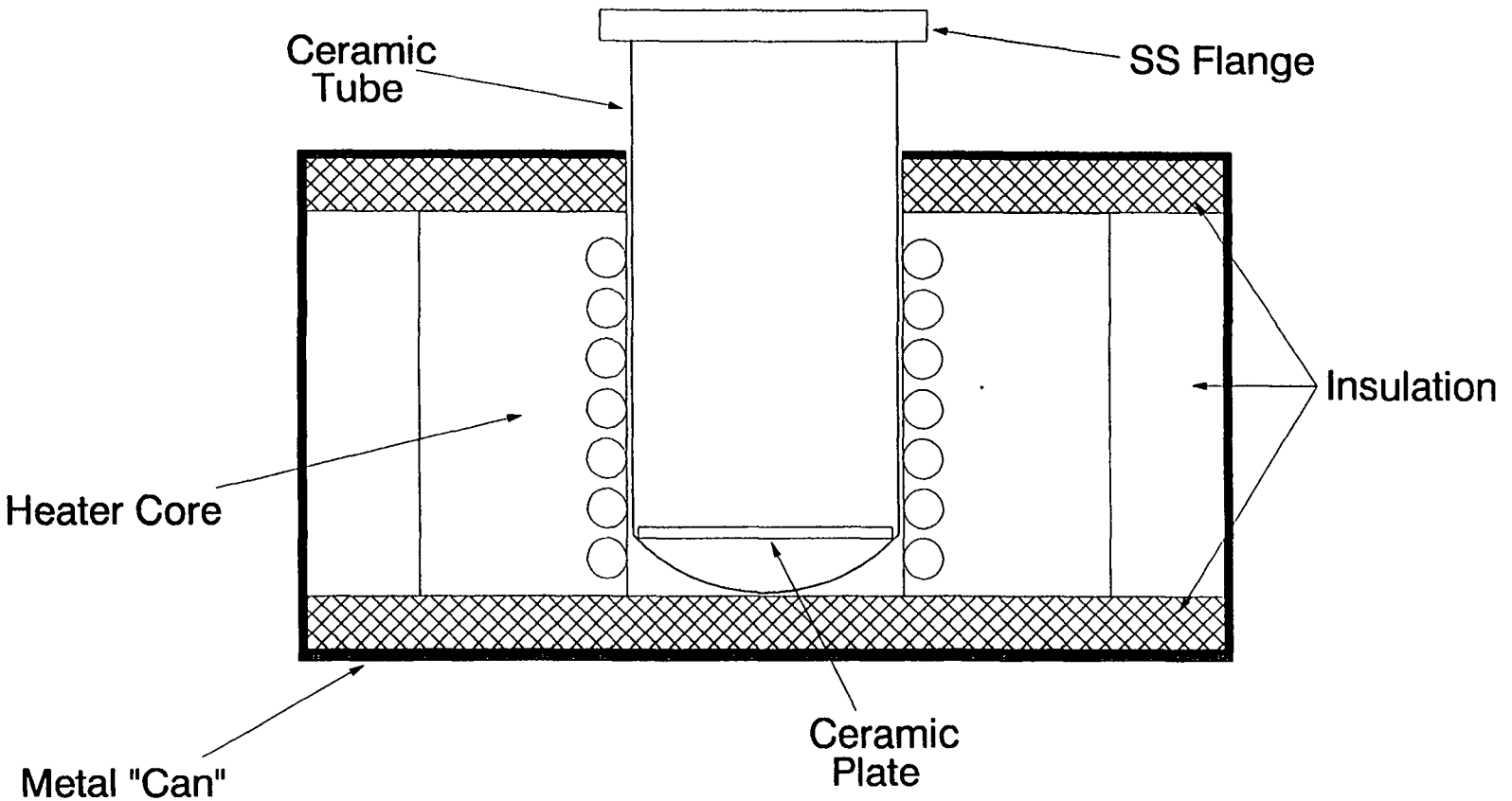

Fig. 18. Modified Apparatus for Oxide Solubility Measurements

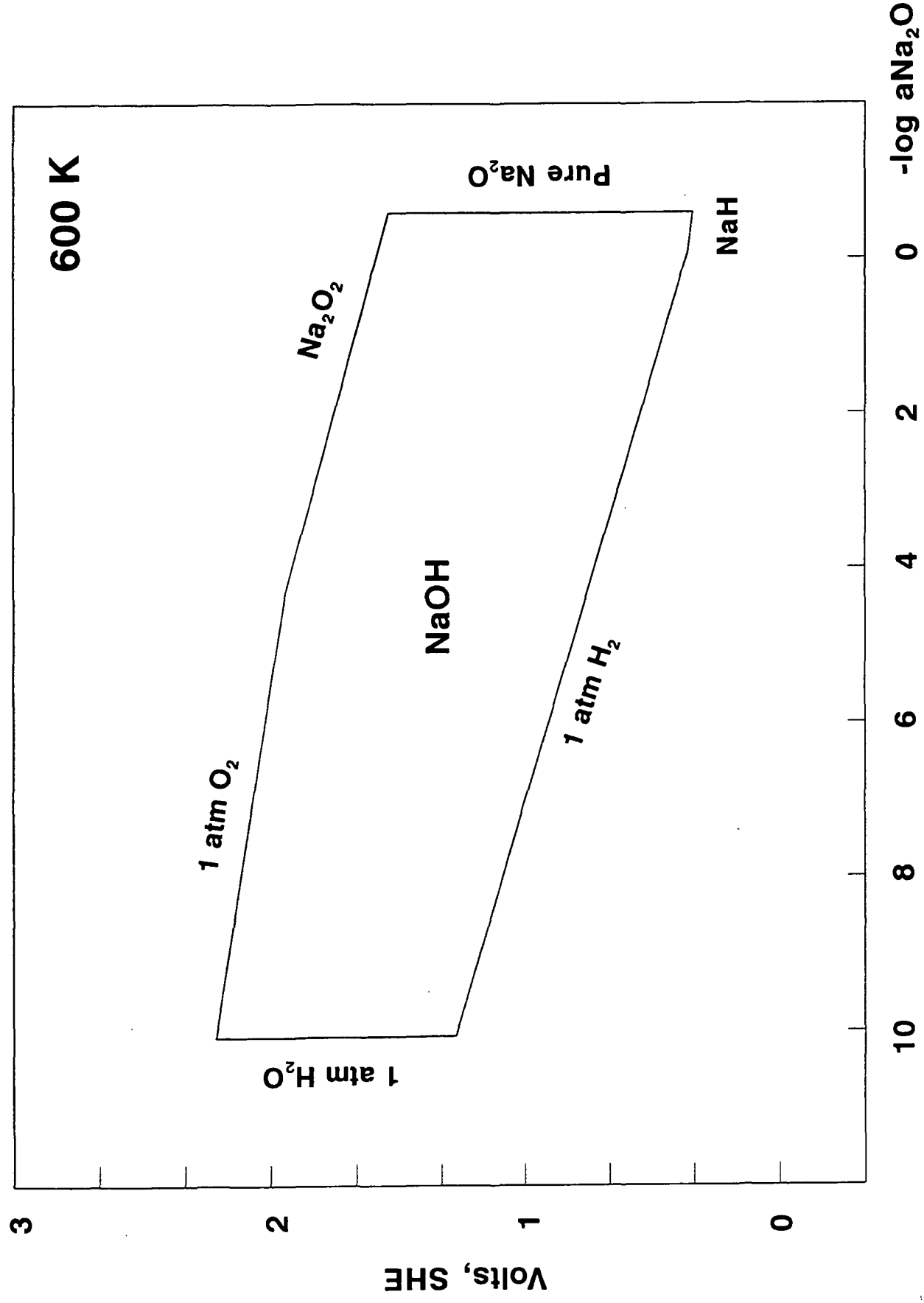

Fig. 19. Potential-Basicity Plot for Stability of NaOH at 600 K

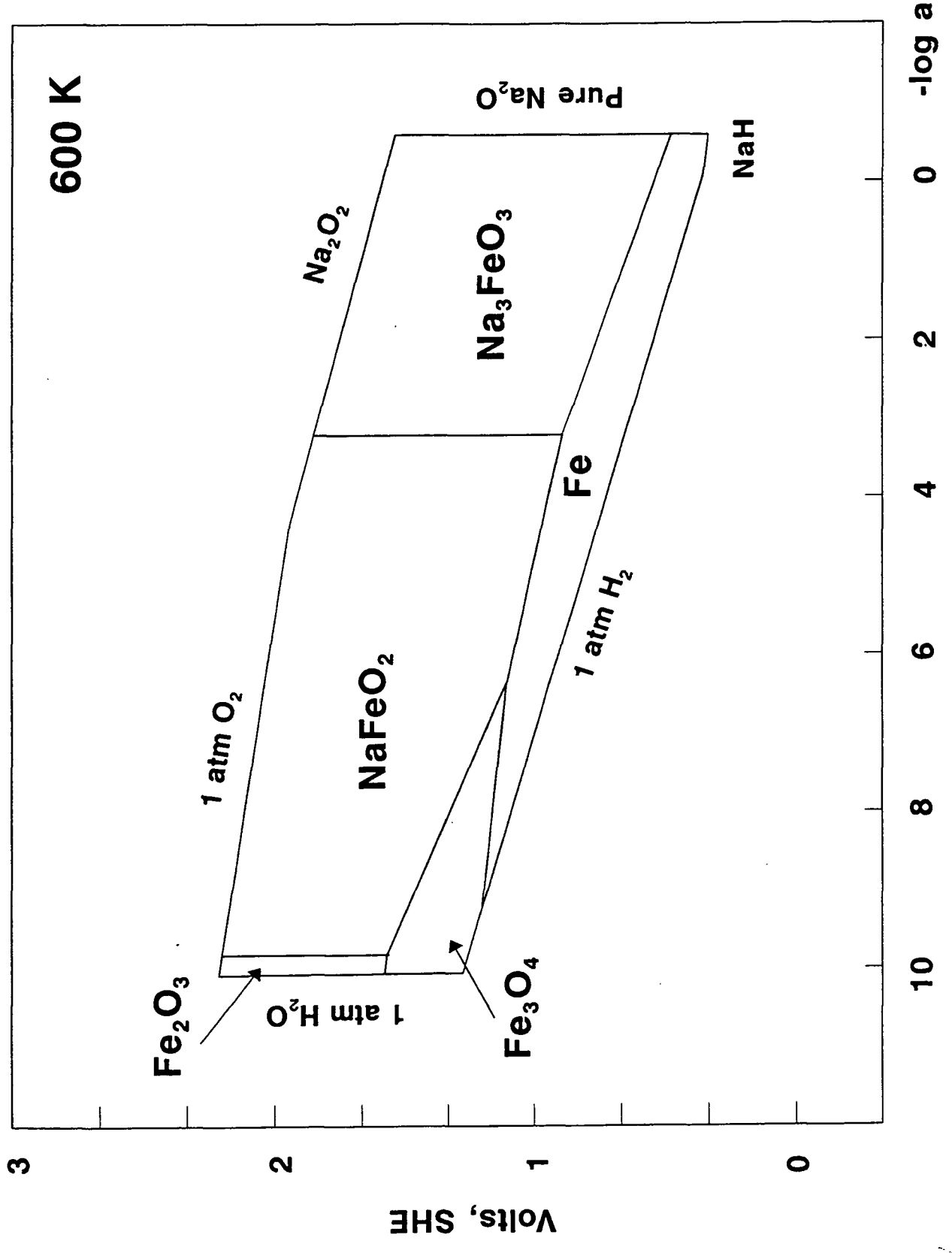

Fig. 20. Potential-Basicity Plot for Stability of Fe in NaOH at 600 K

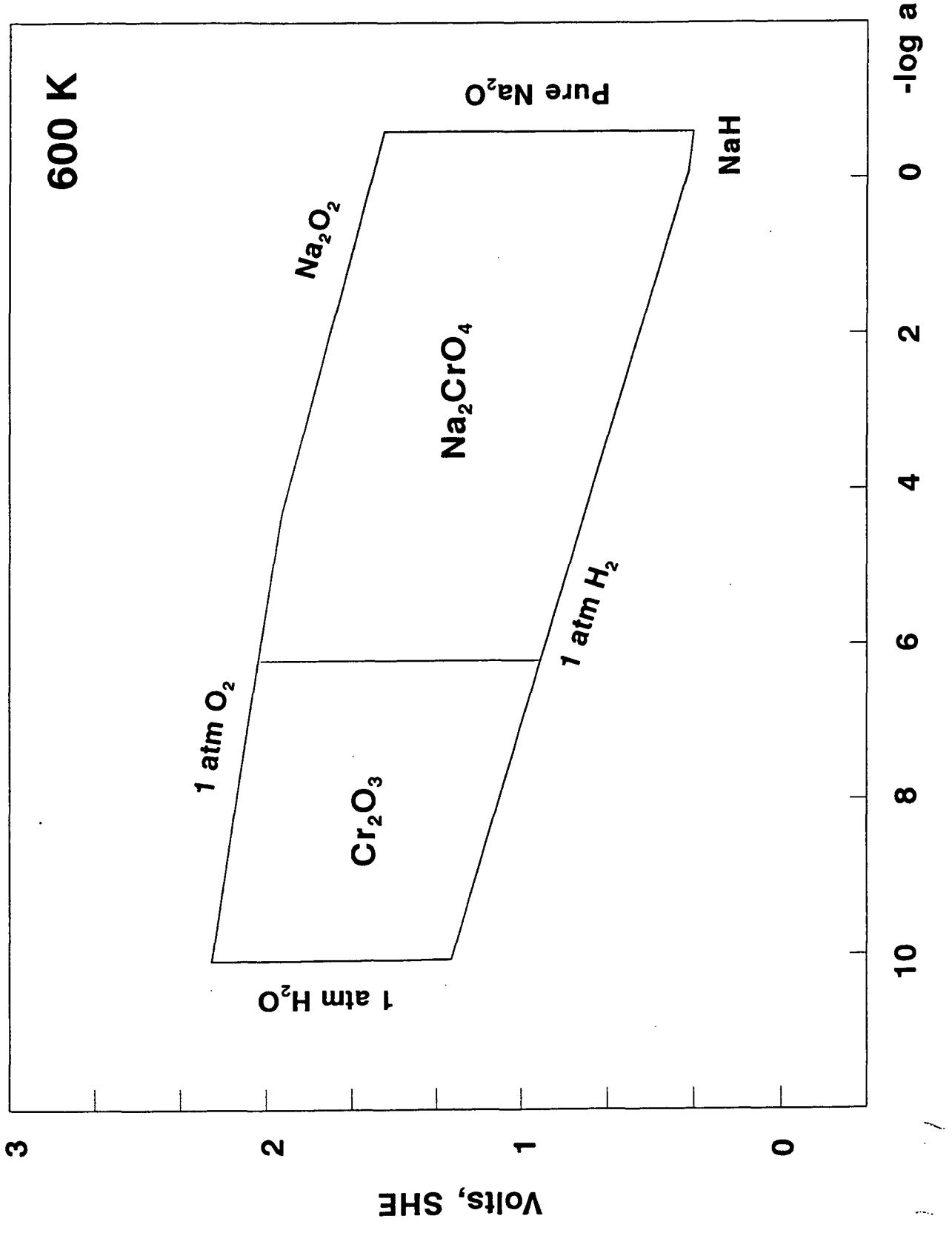

Fig. 21. Potential-Basicity Plot for Stability of Cr in NaOH at 600 K

needs to be confirmed, so the positions of the boundaries may shift to some extent. In any case, the diagrams do serve to show what phases are expected to be stable under the specific conditions of E-pNa_2O. Interesting for Fe is that there is only a very small oxide field of stability expected, which may indicate that carbon steel is not subject to hot corrosion because the oxide is not stable anyway, and that Fe is converted to $NaFeO_2$ directly, which has a low solubility in the melt. For Cr, the oxide is stable over about 4 orders of magnitude in basicity. These plots will be useful in guiding the solubility studies, and will contribute to our overall understanding of the process of air port corrosion.

CONCLUSIONS AND RECOMMENDATIONS

This project is focused on two main areas of corrosion in the lower furnace of the recovery boiler: fireside corrosion and corrosion due to hydroxide condensation at ports. Our understanding of the gas-solid reactions leading to sulfidation of carbon steel tubes has improved with the knowledge of how specific components of the gas impact kinetics. For example, at constant sulfur pressure, the influence of water vapor does not appear to be large. Moreover, it appears that a correlation with oxygen or sulfur dioxide exists, and that at a critical level the kinetics dramatically increase. Our experimental methods are being modified to merge with those being proposed by AFPA so that future data can be directly used by other laboratories.

The need for sensor development is still identified as an important need for furthering our understanding of gas-solid reactions in the recovery boiler. Solid electrolytes based on sulfates offer one possible method, but only provide information on the product of sulfur and oxygen activities. To arrive at a useful measurement of the conditions will require additional independent knowledge of either the sulfur or oxygen activity. Additional efforts this year were spent trying to identify methods to utilize zirconia oxygen sensors at low temperatures, but were not successful. However, a new technique based on the use of AgI as a sulfur sensor may allow development of the sulfate sensors to go forward. This sensor will have a limited range of applicable sulfur pressures, but these values are expected to be close to those needed for recovery boilers.

The initial experiments by Lisa McMillian for her master's research concluded that the current apparatus for measuring continuous kinetics is not accurate. The deposition of components from the complex simulated furnace gas would not allow weight changes to be followed. A brief morphological investigation of the effect of preoxidation showed that at a higher oxygen pressure, the sulfidation kinetics appeared to be slower.

The previous report outlined a postulated mechanism for air port corrosion which was consistent with a number of observations. During last year a new apparatus was built which will facilitate the collection of oxide solubility data in molten hydroxides. An offer was made to a post-doctoral associate to work full-time on this task. He arrived in November, but did not have the proper immigration status, and could not be hired. This task was then taken on by a new Ph.D. student, Matt Estes, who successfully defended his proposal and began work in March of 1993.

FUTURE ACTIVITIES

1. Two of our furnaces used for gas-solid reactions are committed to AFPA-funded work for the next 9 months. We propose to modify our remaining furnace to conduct rapid thermal cycling experiments. This would be accomplished by developing a system to raise and lower a vertically mounted furnace by use of a motor driven pulley. This will allow us to evaluate thermal cycles which are more severe than those which can currently be investigated. Pending the acquisition of additional furnace capacity, further work on the impact of gas composition at constant, but lower, sulfur pressures will be conducted in concert with the AFPA project.

2. Several inquiries on the effect of burning bleach plant effluent will be addressed by developing a report on the current state of understanding of how materials perform in gases containing higher levels of HCl. Environmental calculations will be used in conjunction with the literature on materials for burning high chlorine coal to assess whether further experimentation is needed for this application.

3. A AgI cell will be constructed to determine how it will function in our environments of interest. If it is successful, then a sulfate sensor will be constructed to determine if the local environment can be characterized beneath a frozen smelt layer. By early fall, a new Ph.D. student in corrosion will begin his research, and might be encouraged to take on this project to establish useful ranges, optimize critical parameters, and develop the fundamental understanding of this technology for recovery applications.

4. Work on the oxide solubility measurements will be continued by Matt Estes as part of his Ph.D. studies. Measurements will be made to determine the effect of melt chemistry, acid-base behavior and temperature, and will be used to determine whether the proposed mechanism is realistic. The development of a suitable basicity probe for the laboratory measurements may also be of use for later field measurements.